

Article

# Latest Maastrichtian middle- and high-latitude mosasaurs and fish isotopic composition: carbon source, thermoregulation strategy, and thermal latitudinal gradient

Léa Leuzinger , László Kocsis\* , Zoneibe Luz, Torsten Vennemann, Alexey Ulyanov, and Marta Fernández

**Abstract.**—Here we report high-latitude stable isotope compositions of Maastrichtian fossil fish and marine reptiles (mainly mosasaurs) from Antarctica (64°S paleolatitude) and compare them with mid-paleolatitude samples from Argentine Patagonia (45°S). Disparities between the  $\delta^{13}\text{C}$  values of bony fish and marine reptiles correspond to differences in the foraging ground (distance from the shore and depth), while dramatically higher  $\delta^{13}\text{C}$  values (by 18‰) in shark enameloid cannot be explained through ecology and are here imputed to biomineralization. Comparison with extant vertebrates suggests that the diet alone can explain the offset observed between bony fish and mosasaurs; however, breath holding due to a diving behavior in mosasaurs may have had some impact on their  $\delta^{13}\text{C}$  values, as previously suggested. The  $\delta^{18}\text{O}_{\text{PO}_4}$  values of the remains confirm a relatively stable, elevated body temperature for marine reptiles, meaning that they were thermoregulators. We calculated a water temperature of  $\sim 8^\circ\text{C}$  for Antarctica from the fish  $\delta^{18}\text{O}_{\text{PO}_4}$  values, warmer than present-day temperatures and consistent with the absence of polar ice sheets during the latest Maastrichtian. Our fish data greatly extend the latitudinal range of Late Cretaceous fish  $\delta^{18}\text{O}_{\text{PO}_4}$  values and result in a thermal gradient of  $0.4^\circ\text{C}/1^\circ$  of latitude when combined with literature data.

Léa Leuzinger. Laboratorio de Paleontología de Vertebrados, IDEAN (CONICET), Departamento de Ciencias Geológicas, FCEN, Universidad de Buenos Aires, Intendente Gurría 2160, Ciudad Universitaria–Pabellón II, C1428EGA Ciudad Autónoma de Buenos Aires, Argentina. E-mail: [leuzinger.lea@gmail.com](mailto:leuzinger.lea@gmail.com)

László Kocsis, Zoneibe Luz, and Torsten Vennemann. Institut des Dynamiques de la Surface Terrestre (IDYST), Université de Lausanne, rue de la Mouline, 1015 Lausanne, Switzerland. E-mail: [laszlo.kocsis@unil.ch](mailto:laszlo.kocsis@unil.ch), [zoneibe.luz@gmail.com](mailto:zoneibe.luz@gmail.com), [torsten.Vennemann@unil.ch](mailto:torsten.Vennemann@unil.ch)

Alexey Ulyanov. Institute of Earth Sciences (ISTE), University of Lausanne, rue de la Mouline, 1015 Lausanne, Switzerland. E-mail: [alexey.ulyanov@unil.ch](mailto:alexey.ulyanov@unil.ch)

Marta Fernández. Departamento Paleontología Vertebrados, Museo de La Plata, 1900 La Plata, Argentina. E-mail: [martafer@fcnym.unlp.edu.ar](mailto:martafer@fcnym.unlp.edu.ar)

Accepted: 24 October 2022

\*Corresponding author.

## Introduction

Mosasaur (Lepidosauria, Squamata) fossils have revealed several of their physiological and behavioral traits in the last decades: evidence concerning their endothermy (Bernard et al. 2010; Motani 2010), diving (Schulp et al. 2013), and migration behavior (Lindgren and Siverson 2005) has been presented based on their stable isotope signature. These traits add to environmental drivers that can influence the carbon and oxygen isotope compositions of mosasaur bioapatite, such as the climate,

the food source, their wide latitudinal distribution (see Bernard et al. 2010), and the euryhalinity of some of the taxa (Kocsis et al. 2009). To better understand the relative importance of each of these drivers, we compare the oxygen and carbon stable isotope compositions ( $\delta^{18}\text{O}_{\text{PO}_4}$ ,  $\delta^{18}\text{O}_{\text{CO}_3}$ , and  $\delta^{13}\text{C}$ ) of fish (actinopterygians and chondrichthyans) and plesiosaur bioapatite with those of mosasaurs from two latest Maastrichtian sites of different paleolatitudes, namely the Isla Marambio (Seymour Island), Antarctic Peninsula (64°S), and Los

Bajos de Trapalcó and Santa Rosa, Argentine Patagonia (45°S).

The  $\delta^{13}\text{C}$  composition mainly depends on the food source, which links to dissolved organic and inorganic carbon, both of which vary with latitude, water depth, and distance from the shore (e.g., Goericke and Fry 1994). Differences in the carbon fraction are thus expected between the two sites due to different paleolatitudes, and intertaxonomic differences relating to different habitats might also appear. In addition to diet, other factors may influence the carbon isotope composition of bioapatite: breath holding is thought to lower the  $\delta^{13}\text{C}$  values of pulmonate diving animals such as mosasaurs (Robbins et al. 2008; Schulp et al. 2013, 2017; van Baal et al. 2013), while sharks are known to show particularly high  $\delta^{13}\text{C}$  values in their enameloid (Vennemann et al. 2001; van Baal et al. 2013; Kocsis et al. 2014).

Because  $\delta^{18}\text{O}_{\text{PO}_4}$  values depend strongly on the precipitation temperature of bioapatite (Kolodny et al. 1983), we expect the latitudinal thermal gradient to have a marked influence on the  $\delta^{18}\text{O}_{\text{PO}_4}$  values of thermoconforming taxa (i.e., with a body temperature varying according to the ambient temperature; e.g., Withers 1992), while the  $\delta^{18}\text{O}_{\text{PO}_4}$  values of thermoregulating taxa such as mosasaurs and plesiosaurs (Bernard et al. 2010; Harrell et al. 2016) should be more stable across latitudes. A thorough literature search revealed that stable isotope data of Late Cretaceous marine vertebrates from sites beyond 52° paleolatitude are absent so far, limiting the elaboration of a complete latitudinal thermal gradient based on thermoconforming vertebrates (e.g., Pucéat et al. 2007). Our fish values greatly extend the latitudinal range of marine vertebrate  $\delta^{18}\text{O}_{\text{PO}_4}$  data, and we explore here their implication for global latitudinal gradients elaborated so far.

### Geographic, Geological, and Climatic Background

The material studied comes from two geographic areas: Río Negro Province, northern Argentine Patagonia; and Marambio (i.e., Seymour) Island, Antarctic Peninsula (Fig. 1). Photographs of the material are available in the Supplementary Material.

Río Negro Province, Argentine Patagonia

The Patagonian material was recovered from the sites of Los Bajos de Trapalcó and Santa Rosa, Río Negro Province (Argentina), and is assigned to the latest Cretaceous Jagüel Formation, which is part of the Malargüe Group. During the Campanian–Maastrichtian, northern Patagonia was an archipelago largely flooded by the Atlantic Ocean as a consequence of sediment load and thermal subsidence of the lithosphere (Uliana and Biddle 1988; Gasparini et al. 2001). During that period, the volcanic arc related to the Andean orogeny was developing to the west. In the study area, the Jagüel Formation deposited under marine settings at the southern margin of the Neuquén Basin (Gasparini et al. 2003; O’Gorman et al. 2014) and mostly consists of olive-green mudstones, occasionally laminated (Gasparini et al. 2003; Fernández et al. 2008). The Cretaceous/Paleogene boundary (K/Pg) is contained within the Jagüel Formation, as evidenced by the presence of late Maastrichtian nannofossils followed by *Biantholithus sparsus*, an index nannofossil for the early Danian (Fernández et al. 2008).

Isla Marambio, Antarctic Peninsula

The Antarctic material comes from a unit of the López de Bertodano Formation (LBF) (Rinaldi et al. 1978), a homoclinal sequence dipping 8° to 10° toward the east (Macellari 1988) and extending SSW–NNE at the center of Isla Marambio, itself located east of the Antarctic Peninsula. The LBF constitutes the uppermost part of the Santonian–Danian Marambio Group (Olivero 2012), and it is Maastrichtian to Danian in age (González Ruiz et al. 2019). It was deposited in the back-arc Larsen Basin (James Ross subbasin), east of the active arc of the Antarctic Peninsula generated by the subduction of the proto-Pacific oceanic crust (Ditchfield et al. 1994). The LBF is divided into two sections, the “lower *Rotularia* units” and the “upper molluscan units,” and 10 informal units (LB1 to LB10) defined by Macellari (1988), the first of which has since been reassigned to an older formation (see González Ruiz et al. 2019). The study material comes from the ninth unit (Unit 9), which includes a glauconite-rich interval that contains the K/Pg boundary, characterized by a reduction of the number of invertebrate fossils, a

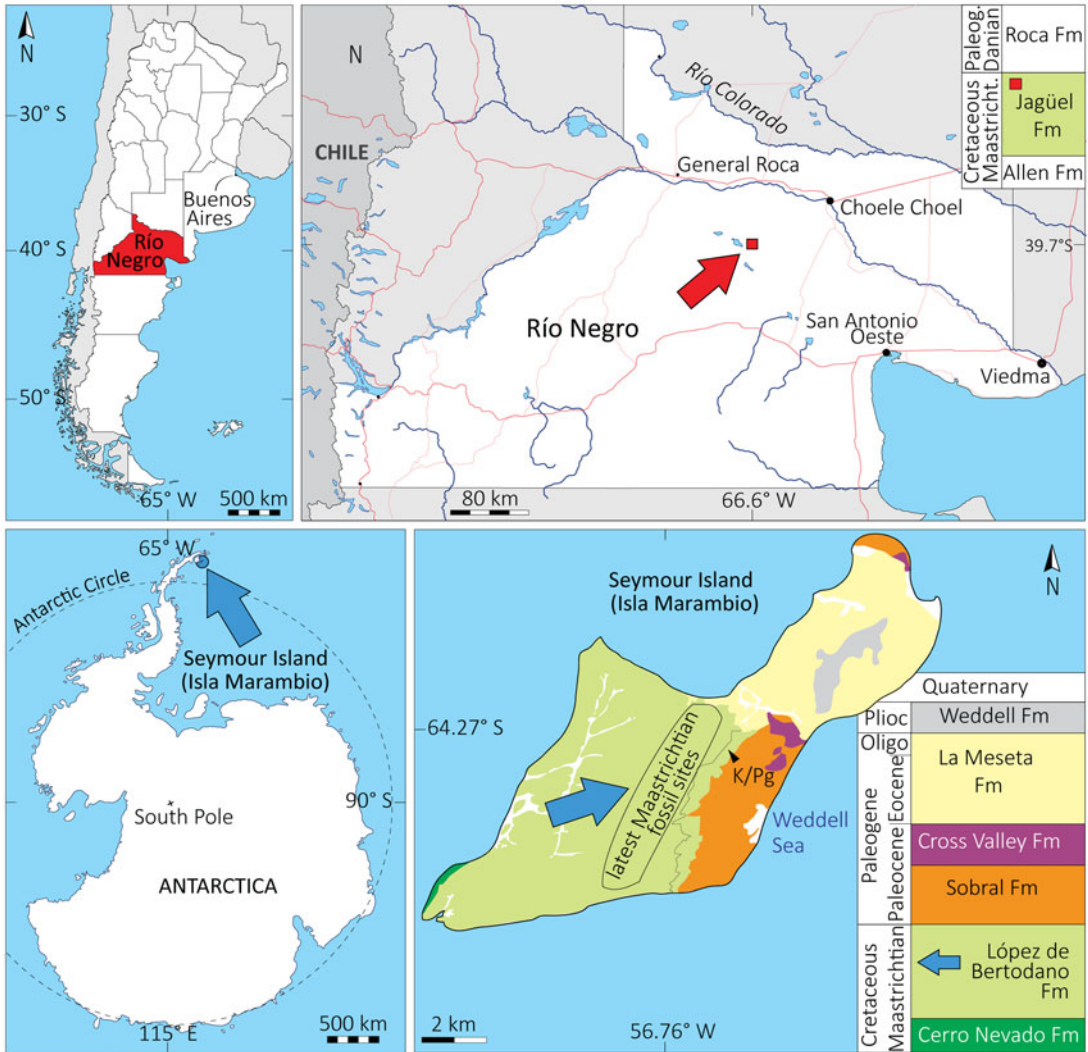


FIGURE 1. Geographic and stratigraphic setting of the study sites. A, Los Bajos de Trapalcó and Santa Rosa, Río Negro Province, Argentine Patagonia. B, Isla Marambio (Seymour Island), Antarctic Peninsula. Based on Montes et al. (2007), Fernández et al. (2008), and Fernández and Gasparini (2012). Oligo, Oligocene; Paleog, Paleogene; Plioc, Pliocene.

sudden lack of ammonites, and an iridium anomaly (Elliot et al. 1994). According to sedimentological studies, the sandy siltstones of Unit 9 were deposited in a shallow outer shelf under low-energy settings and below the wave base (Macellari 1988; Elliot et al. 1994). An upward-increasing abundance of glauconite across Unit 9 suggests an increase in water depth with time. This unit reflects a marine transgression and represents the deepest, most offshore facies of the LBF (Macellari 1988; O’Gorman et al. 2020), in the general context

of a prograding shelf that characterizes the Marambio Group (Olivero 2012).

#### Climatic Context

The Cretaceous Period is considered one of the warmest of Earth’s history, although numerous studies point to a global cooling by the Campanian based on different paleothermometers ( $\delta^{18}\text{O}$  of foraminifera,  $\text{TEX}_{86}$ ; Li and Keller 1998; Linnert et al. 2014). The last 200 kyr of the Maastrichtian in particular appear to have been a relatively cooler period within

the Cretaceous, still with no evidence of permanent ice sheets near the poles. At a smaller spatial and temporal scale, a multi-proxy analysis has suggested a gradual warming at the end of the Maastrichtian in the South Atlantic region (Woelders et al. 2017). The absence of large ice masses resulted in seawater  $\delta^{18}\text{O}$  estimated to be equal to  $-1\text{‰}$  (Shackleton and Kennett 1976), that is, lower than the present value ( $0\text{‰}$  on average). A seawater  $\delta^{18}\text{O}$  value of  $-1.25\text{‰}$  is also reported for the Late Cretaceous in particular (Pucéat et al. 2007). The thermal latitudinal gradient, closely related to the atmospheric  $p\text{CO}_2$ , was shallower during the Cretaceous than it is today (present gradient =  $0.56^\circ\text{C}/1^\circ$  of latitude; Zhang et al. 2019); however, it became steeper by the end of the period due to a decrease of  $p\text{CO}_2$  in the atmosphere (Linnert et al. 2014). For the last period of the Maastrichtian, Zhang et al. (2019) published a marine latitudinal gradient of  $0.41^\circ\text{C}/1^\circ$  of latitude, similar to the terrestrial air temperature gradient of  $0.4^\circ\text{C}/1^\circ$  of latitude calculated by Amiot et al. (2004) based on  $\delta^{18}\text{O}$  values of continental vertebrate bioapatite. Pucéat et al. (2007) also reported a marine latitudinal gradient similar to the present-day gradient for paleolatitudes between  $1^\circ$  and  $50^\circ$ , based on  $\delta^{18}\text{O}$  values of Late Cretaceous fish teeth. This shallower gradient implies that the latitudinal limits of the climate zones were shifted poleward in comparison with present-day zones, and according to Zhang et al. (2019), both of the sites analyzed in our study were located in the temperate climate zone. The paleolatitudes were approximately  $45^\circ\text{S}$  for Patagonian study sites and  $64^\circ\text{S}$  for the Antarctic locality based on the work of van Hinsbergen et al. (2015).

## Material and Methods

### Material

The study material consists of 29 fossil specimens, mainly teeth of mosasaurs, as well as plesiosaurs, bony fish, and sharks from Argentine Patagonia (Los Bajos de Trapalcó and Santa Rosa localities, Río Negro Province) and Antarctica (Unit 9, LBF, Isla Marambio). Among these, 2 mosasaur and 4 shark teeth are from Patagonia, while 15 mosasaur teeth (for one

specimen, an associated bone fragment was also studied), 5 plesiosaur teeth, and 3 bony fish teeth come from Antarctica. The mosasaur material is assigned to Mosasauridae, although some specimens permit a higher degree of taxonomic assignment, such as cf. *Liodon*, *Globidensini*, ?*Plioplatecarpinae* and ?*Mosasaurus* (Table 1). The plesiosaur specimens are referred to the family Elasmosauridae or Aristonectidae. The bony fish material is likely referable to Ichthyodectiformes or Aulopiformes, showing affinities to *Enchodus*. The shark teeth are assigned to the order Lamniformes and probably to the family Odontaspidae.

When possible, we sampled both enamel(oid) and dentine from the same tooth to determine the degree of preservation. In one case (ARG-2, mosasaur), we additionally sampled the bone in which the tooth was still implanted. Every sample was analyzed for the stable isotope composition of its bioapatite carbonate fraction ( $\delta^{13}\text{C}$ ,  $\delta^{18}\text{O}_{\text{CO}_3}$ ), and most were analyzed for their phosphate ( $\delta^{18}\text{O}_{\text{PO}_4}$ ) fraction as well. A selection of samples were also analyzed to determine their rare earth element (REE) concentration. The material from Antarctica was found isolated and loose in the sediment, with the single exception of ARG-1, which was found embedded in a rock concretion. Most of the material used in this study was either completely used up for the analyses, or a small amount of sample powder and/or tiny fragments kept in epoxy remained. However, many fossils from the same sample lot related to the field surveys are kept under the same collection number at the Museo de La Plata in Argentina. These “MLP” catalogue numbers have been provided in Table 1 to allow scientists to examine and resample these faunas for possible future studies.

### Stable Isotope Analyses

We performed carbon and oxygen stable isotope analyses on both the phosphate and structural carbonate fractions of bioapatite at the Stable Isotope Lab of the Institute of Earth Surface Dynamics, University of Lausanne (UNIL), Switzerland. For the analysis of the phosphate fraction ( $\delta^{18}\text{O}_{\text{PO}_4}$ ), we pretreated at least 2 mg of each sample according to the procedure described in Koch et al. (1997), and we

TABLE 1. Oxygen and carbon stable isotope compositions of the study material, measured in phosphate and structural carbonate of bioapatite. bo, bone; td, tooth dentine; te, tooth enamel; VPDB, Vienna Pee Dee Belemnite; VSMOW, Vienna Standard Mean Ocean Water.

| Collection no.  | ID      | Taxon 1      | Taxon 2                          | Site                      | Paleolatitude (°S) | Tissue | $\delta^{13}\text{C}_{\text{CO}_3}$ |     | $\delta^{18}\text{O}_{\text{CO}_3}$ |     | $\delta^{18}\text{O}_{\text{PO}_4}$ |         |     |
|-----------------|---------|--------------|----------------------------------|---------------------------|--------------------|--------|-------------------------------------|-----|-------------------------------------|-----|-------------------------------------|---------|-----|
|                 |         |              |                                  |                           |                    |        | ‰ VPDB                              | SD  | ‰ VPDB                              | SD  | ‰ VSMOW                             | ‰ VSMOW | SD  |
| MLP 15-I-24-41a | ARG-1   | Mosasauria   | cf. <i>Liodon</i>                | Isla Marambio, Antarctica | 64                 | te     | -8.2                                | 0.0 | -4.0                                | 0.2 | 26.8                                | 18.9    | 0.1 |
|                 | ARG-1   | Mosasauria   | cf. <i>Liodon</i>                | Isla Marambio, Antarctica | 64                 | td     | -7.8                                | 0.1 | -4.2                                | 0.2 | 26.6                                | 18.1    | 0.0 |
| MLP 15-I-24-41b | ARG-2   | Mosasauria   | cf. <i>Liodon</i>                | Isla Marambio, Antarctica | 64                 | bo     | -14.0                               | 0.1 | -0.6                                | 0.1 | 30.3                                | -       | -   |
| MLP 15-I-24-44  | ARG-3   | Mosasauria   | Globidensini                     | Isla Marambio, Antarctica | 64                 | te     | -11.2                               | 0.0 | -4.6                                | 0.2 | 26.2                                | 18.9    | 0.1 |
|                 | ARG-3   | Mosasauria   | Globidensini                     | Isla Marambio, Antarctica | 64                 | td     | -3.4                                | 0.0 | -2.9                                | 0.1 | 27.9                                | -       | -   |
| MLP 15-I-24-48  | ARG-4   | Mosasauria   | indet.                           | Isla Marambio, Antarctica | 64                 | te     | -11.8                               | 0.1 | -4.4                                | 0.2 | 26.4                                | 19.1    | 0.0 |
|                 | ARG-4   | Mosasauria   | indet.                           | Isla Marambio, Antarctica | 64                 | td     | -6.8                                | 0.0 | -3.1                                | 0.1 | 27.7                                | -       | -   |
| MLP 15-I-24-33a | ARG-5   | Mosasauria   | cf. <i>Liodon</i>                | Isla Marambio, Antarctica | 64                 | te     | -13.5                               | 0.1 | -3.9                                | 0.2 | 26.9                                | 19.3    | 0.0 |
|                 | ARG-5   | Mosasauria   | cf. <i>Liodon</i>                | Isla Marambio, Antarctica | 64                 | td     | -11.2                               | 0.0 | -2.4                                | 0.1 | 28.4                                | 21.8    | 0.1 |
|                 | ARG-5   | Mosasauria   | cf. <i>Liodon</i>                | Isla Marambio, Antarctica | 64                 | te     | -11.4                               | 0.1 | -3.6                                | 0.1 | 27.2                                | -       | -   |
| MLP 15-I-24-29  | ARG-8   | Mosasauria   | ?Plioplatecarpinae               | Isla Marambio, Antarctica | 64                 | te     | -10.6                               | 0.1 | -4.8                                | 0.1 | 25.9                                | 19.0    | 0.2 |
|                 | ARG-8   | Mosasauria   | ?Plioplatecarpinae               | Isla Marambio, Antarctica | 64                 | td     | -9.3                                | 0.1 | -2.8                                | 0.2 | 28.1                                | -       | -   |
| MLP 15-I-24-55a | ARG-10  | Mosasauria   | ?Plioplatecarpinae               | Isla Marambio, Antarctica | 64                 | te     | -6.8                                | 0.0 | -4.8                                | 0.2 | 25.9                                | 20.0    | 0.3 |
|                 | ARG-10  | Mosasauria   | ?Plioplatecarpinae               | Isla Marambio, Antarctica | 64                 | td     | -1.9                                | 0.0 | -4.0                                | 0.2 | 26.8                                | -       | -   |
| MLP 13-XI-29-1  | ARG-12A | Mosasauria   | indet.                           | Isla Marambio, Antarctica | 64                 | te     | -10.6                               | 0.0 | -4.9                                | 0.2 | 25.9                                | 18.5    | 0.0 |
|                 | ARG-12A | Mosasauria   | indet.                           | Isla Marambio, Antarctica | 64                 | td     | -3.5                                | 0.0 | -3.3                                | 0.1 | 27.5                                | -       | -   |
|                 | ARG-12B | Mosasauria   | indet.                           | Isla Marambio, Antarctica | 64                 | te     | -10.5                               | 0.1 | -2.6                                | 0.2 | 28.2                                | 20.9    | 0.2 |
| MLP 15-I-24-25  | ARG-12B | Mosasauria   | indet.                           | Isla Marambio, Antarctica | 64                 | td     | -7.9                                | 0.1 | -3.2                                | 0.2 | 27.6                                | -       | -   |
|                 | ARG-13  | Mosasauria   | cf. <i>Liodon</i>                | Isla Marambio, Antarctica | 64                 | te     | -11.8                               | 0.1 | -3.5                                | 0.3 | 27.3                                | 20.1    | 0.3 |
| MLP 15-I-24-33b | ARG-13  | Mosasauria   | cf. <i>Liodon</i>                | Isla Marambio, Antarctica | 64                 | td     | -5.7                                | 0.0 | -3.4                                | 0.2 | 27.4                                | 21.8    | 0.4 |
|                 | ARG-14  | Mosasauria   | cf. <i>Liodon</i>                | Isla Marambio, Antarctica | 64                 | te     | -12.5                               | 0.1 | -2.6                                | 0.2 | 28.2                                | 21.4    | 0.3 |
| MLP 15-I-24-30  | ARG-14  | Mosasauria   | cf. <i>Liodon</i>                | Isla Marambio, Antarctica | 64                 | td     | -6.6                                | 0.1 | -3.6                                | 0.2 | 27.2                                | -       | -   |
|                 | ARG-15  | Mosasauria   | indet.                           | Isla Marambio, Antarctica | 64                 | te     | -15.4                               | 0.1 | -3.5                                | 0.2 | 27.3                                | 20.5    | 0.3 |
|                 | ARG-15  | Mosasauria   | indet.                           | Isla Marambio, Antarctica | 64                 | td     | -7.7                                | 0.0 | -3.5                                | 0.2 | 27.3                                | -       | -   |
|                 | ARG-20  | Mosasauria   | indet.                           | Isla Marambio, Antarctica | 64                 | te     | -                                   | -   | -                                   | -   | -                                   | 21.0    | 0.1 |
|                 | ARG-20  | Mosasauria   | indet.                           | Isla Marambio, Antarctica | 64                 | td     | -4.2                                | 0.0 | -3.5                                | 0.1 | 27.3                                | 22.1    | 0.1 |
|                 | ARG-21  | Mosasauria   | indet.                           | Isla Marambio, Antarctica | 64                 | td     | -4.4                                | 0.0 | -2.8                                | 0.1 | 28.0                                | 21.2    | 0.1 |
|                 | ARG-22  | Mosasauria   | indet.                           | Isla Marambio, Antarctica | 64                 | te     | -11.9                               | 0.0 | -2.9                                | 0.1 | 27.9                                | 19.6    | 0.8 |
|                 | ARG-22  | Mosasauria   | indet.                           | Isla Marambio, Antarctica | 64                 | td     | -4.1                                | 0.0 | -3.5                                | 0.0 | 27.3                                | 20.7    | 0.1 |
| MLP 15-I-24-41c | ARG-6   | Plesiosauria | Elasmosauridae or Aristonectidae | Isla Marambio, Antarctica | 64                 | te     | -11.8                               | 0.1 | -4.3                                | 0.2 | 26.5                                | 19.1    | 0.2 |
|                 | ARG-6   | Plesiosauria | Elasmosauridae or Aristonectidae | Isla Marambio, Antarctica | 64                 | td     | -5.5                                | 0.0 | -3.5                                | 0.1 | 27.3                                | -       | -   |
| MLP 15-I-24-56  | ARG-7   | Plesiosauria | Elasmosauridae or Aristonectidae | Isla Marambio, Antarctica | 64                 | te     | -10.5                               | 0.1 | -5.9                                | 0.1 | 24.9                                | 17.0    | 0.3 |
|                 | ARG-7   | Plesiosauria | Elasmosauridae or Aristonectidae | Isla Marambio, Antarctica | 64                 | td     | -7.0                                | 0.0 | -4.3                                | 0.2 | 26.5                                | -       | -   |

Table 1. Continued.

| Collection no.  | ID         | Taxon 1        | Taxon 2                                   | Site                          | Paleolatitude<br>(°S) | Tissue | $\delta^{13}\text{C}_{\text{CO}_3}$ |      | $\delta^{18}\text{O}_{\text{CO}_3}$ |      | $\delta^{18}\text{O}_{\text{CO}_3}$ |         | $\delta^{18}\text{O}_{\text{PO}_4}$ |    |
|-----------------|------------|----------------|---|-------------------------------|-----------------------|--------|-------------------------------------|------|-------------------------------------|------|-------------------------------------|---------|-------------------------------------|----|
|                 |            |                |   |                               |                       |        | ‰ VPDB                              | SD   | ‰ VPDB                              | SD   | ‰ VSMOW                             | ‰ VSMOW | SD                                  | SD |
| MLP 13-XI-29-24 | ARG-9A     | Plesiosauria   | Elasmosauridae or<br>Aristonectidae       | Isla Marambio, Antarctica     | 64                    | te     | -11.6                               | 0.1  | -4.7                                | 0.2  | 26.1                                | 16.9    | 0.2                                 |    |
|                 | ARG-9A     | Plesiosauria   | Elasmosauridae or<br>Aristonectidae       | Isla Marambio, Antarctica     | 64                    | td     | -7.5                                | 0.1  | -2.2                                | 0.2  | 28.6                                | -       | -                                   |    |
|                 | ARG-9B     | Plesiosauria   | Elasmosauridae or<br>Aristonectidae       | Isla Marambio, Antarctica     | 64                    | te     | -12.5                               | 0.0  | -1.7                                | 0.2  | 29.2                                | 20.3    | 0.3                                 |    |
|                 | ARG-9B     | Plesiosauria   | Elasmosauridae or<br>Aristonectidae       | Isla Marambio, Antarctica     | 64                    | td     | -5.6                                | 0.1  | -3.0                                | 0.2  | 27.8                                | -       | -                                   |    |
|                 | ARG-9C     | Plesiosauria   | Elasmosauridae or<br>Aristonectidae       | Isla Marambio, Antarctica     | 64                    | te     | -12.7                               | 0.1  | -3.0                                | 0.2  | 27.8                                | 19.6    | 0.1                                 |    |
|                 | ARG-9C     | Plesiosauria   | Elasmosauridae or<br>Aristonectidae       | Isla Marambio, Antarctica     | 64                    | td     | -7.8                                | 0.1  | -1.5                                | 0.2  | 29.4                                | 19.7    | 0.1                                 |    |
| MLP 13-XI-19-38 | ARG-16A    | Actinopterygii | Ichthyodectiformes or<br>Aulopiformes     | Isla Marambio, Antarctica     | 64                    | te     | -4.5                                | 0.1  | -1.4                                | 0.2  | 29.5                                | 23.2    | 0.5                                 |    |
|                 | ARG-16A    | Actinopterygii | Ichthyodectiformes or<br>Aulopiformes     | Isla Marambio, Antarctica     | 64                    | td     | 4.5                                 | 0.1  | -3.7                                | 0.2  | 27.1                                | 22.6    | 0.4                                 |    |
|                 | ARG-16B    | Actinopterygii | Ichthyodectiformes or<br>Aulopiformes     | Isla Marambio, Antarctica     | 64                    | te     | -5.4                                | 0.1  | -1.9                                | 0.2  | 29.0                                | 23.0    | 0.0                                 |    |
|                 | ARG-16B    | Actinopterygii | Ichthyodectiformes or<br>Aulopiformes     | Isla Marambio, Antarctica     | 64                    | td     | 2.9                                 | 0.1  | -3.2                                | 0.2  | 27.6                                | -       | -                                   |    |
|                 | ARG-16C    | Actinopterygii | Ichthyodectiformes or<br>Aulopiformes     | Isla Marambio, Antarctica     | 64                    | te     | -4.4                                | 0.1  | -1.1                                | 0.2  | 29.8                                | 23.1    | 0.1                                 |    |
|                 | ARG-16C    | Actinopterygii | Ichthyodectiformes or<br>Aulopiformes     | Isla Marambio, Antarctica     | 64                    | td     | 3.1                                 | 0.1  | -3.6                                | 0.2  | 27.2                                | -       | -                                   |    |
|                 | ARG-17A    | Chondrichthyes | Lamniformes                               | Río Negro Province, Argentina | 45                    | te     | 6.6                                 | 0.1  | -4.6                                | 0.2  | 26.2                                | 22.1    | 0.2                                 |    |
|                 | ARG-17A    | Chondrichthyes | Lamniformes                               | Río Negro Province, Argentina | 45                    | td     | -1.6                                | 0.0  | -5.1                                | 0.3  | 25.6                                | 19.4    | 0.1                                 |    |
|                 | ARG-17B    | Chondrichthyes | Lamniformes                               | Río Negro Province, Argentina | 45                    | te     | 6.4                                 | 0.1  | -5.0                                | 0.1  | 25.7                                | 21.6    | 0.1                                 |    |
|                 | ARG-17B    | Chondrichthyes | Lamniformes                               | Río Negro Province, Argentina | 45                    | td     | -0.7                                | 0.1  | -5.5                                | 0.2  | 25.3                                | -       | -                                   |    |
|                 | ARG-17C    | Chondrichthyes | Lamniformes                               | Río Negro Province, Argentina | 45                    | te     | 6.0                                 | 0.0  | -5.4                                | 0.2  | 25.3                                | 22.4    | 0.2                                 |    |
|                 | ARG-17C    | Chondrichthyes | Lamniformes                               | Río Negro Province, Argentina | 45                    | td     | -0.9                                | 0.1  | -5.1                                | 0.2  | 25.7                                | 22.0    | 0.2                                 |    |
|                 | ARG-17D    | Chondrichthyes | Lamniformes                               | Río Negro Province, Argentina | 45                    | te     | 9.8                                 | 0.1  | -5.0                                | 0.1  | 25.7                                | -       | -                                   |    |
|                 | ARG-17D    | Chondrichthyes | Lamniformes                               | Río Negro Province, Argentina | 45                    | td     | -1.2                                | 0.0  | -5.0                                | 0.1  | 25.7                                | -       | -                                   |    |
|                 | ARG-18     | Mosasauria     | ? <i>Mosasaurus</i> or ?<br><i>Liodon</i> | Río Negro Province, Argentina | 45                    | te     | -11.1                               | 0.1  | -5.1                                | 0.2  | 25.6                                | 19.8    | 0.0                                 |    |
|                 | ARG-18     | Mosasauria     | ? <i>Mosasaurus</i> or ?<br><i>Liodon</i> | Río Negro Province, Argentina | 45                    | td     | -2.8                                | 0.1  | -4.4                                | 0.2  | 26.4                                | 21.0    | 0.2                                 |    |
| ARG-19          | Mosasauria | indet.         | Río Negro Province, Argentina             | 45                            | te                    | -11.1  | 0.0                                 | -4.2 | 0.0                                 | 26.6 | 18.5                                | 0.1     |                                     |    |
| ARG-19          | Mosasauria | indet.         | Río Negro Province, Argentina             | 45                            | td                    | -3.6   | 0.0                                 | -3.8 | 0.1                                 | 27.0 | 20.3                                | 0.0     |                                     |    |

separated the  $\text{PO}_4^{3-}$  ion from the apatite to precipitate it as silver phosphate (Kocsis 2011; O'Neil et al. 1994). We prepared in parallel the internationally accepted and frequently analyzed NBS-120c phosphorite reference material. A combination of two USGS standards (USGS 80: 12.50‰; and USGS 81: 34.71‰) and two in-house phosphate standards (LK-2L: 12.1‰; and LK-3L: 17.9‰) were used for data reduction. Note that the values were derived by analyzing the standards with a fluorination method (see Vennemann et al. 2002) and/or through calibration with other silver-phosphate standards with a high-temperature conversion elemental analyzer (TC/EA). When possible, we measured triplicates of each sample. The measurement was achieved through a TC/EA coupled to a Finnigan MAT Delta Plus XL mass spectrometer (see Vennemann et al. 2002). The results are expressed in per mille and reported as  $\delta^{18}\text{O}_{\text{PO}_4}$  on the Vienna Standard Mean Ocean Water (VSMOW) scale. The overall analytical error is considered to be 0.3‰; however, most samples often reproduced better, while some others present a higher standard deviation. The NBS-120c yielded an average value of  $22.0 \pm 0.2\%$  ( $n = 6$ ), slightly higher than the value of 21.7‰ generally considered (e.g., O'Neil et al. 1994), but within the analytical error of the method.

The measurement of the carbon and oxygen isotope compositions in the carbonate fraction ( $\delta^{13}\text{C}$  and  $\delta^{18}\text{O}_{\text{CO}_3}$ ) was achieved using a Gasbench II coupled to a Finnigan MAT Delta Plus XL mass spectrometer at UNIL. The equivalent of 10–15  $\mu\text{g}$  of carbonate powder was weighed from each sample. For the normalization of the results, we used an in-house Carrara calcite marble standard calibrated against NBS-19. The  $\delta^{13}\text{C}$  values are expressed relative to the Vienna Pee Dee Belemnite (VPDB), while the  $\delta^{18}\text{O}_{\text{CO}_3}$  values are expressed against the VSMOW scale. The analytical precision for this method was better than  $\pm 0.07\%$  for C isotopes and  $\pm 0.09\%$  for O isotopes.

Expected differences in the isotopic compositions between taxa and sites are used to evaluate the preservation state of the original isotopic composition of our material. Additionally, the sampling is designed to allow the comparison between tissues or ions of differential resistance

to diagenesis (dentine vs. enamel/enameloid, respective carbonate vs. phosphate) and to help detect diagenetic trends.

#### REE Analyses

Selected samples were analyzed for trace element concentrations by laser ablation inductively coupled plasma mass spectrometry (LA-ICP-MS) using a Perkin Elmer ELAN DRC II ICP-MS mass spectrometer at the Institute of Earth Sciences at UNIL, according to the method detailed in Günther et al. (1997). Fragments of fossil teeth and bone were embedded in resin and polished before measurements were made. Each sample was ablated at three to seven spots (diameter = 50–80  $\mu\text{m}$ ). Standard reference material (NIST612) was used for external standardization (Pearce et al. 1997), while CaO was used as an internal standard with values of 54 and 50 wt.%, respectively, for enameloid and for dentine and bone (e.g., Kocsis et al. 2014). Though CaO content may vary within the remains with small deviation from these internal values, the data still allow relative comparison between samples in their normalized REE distributions and elemental ratios. The analytical reproducibility was generally better than  $\pm 5\%$  SE.

We focused on elements that typically have an early diagenetic origin, such as REE and uranium (e.g., Trueman and Tuross 2002) in order to test depositional/burial conditions. However, concentration of other elements such as Cu, Zn, Sr, and Ba are reported as well (see Supplementary Table 1). The data are separated based on the different histological parts such as enamel/enameloid, dentine, and in one case also bone. The REE data are reported normalized to Post Archean Australian Shale (PAAS); and the REE series is subdivided into light (LREE), middle (MREE), and heavy (HREE) elements as follows: LREE (La, Pr, Ce, Nd), MREE (Eu, Gd, Tb, Dy), and HREE (Er, Tm, Yb, Lu). MREE\* is defined by the average of LREE and HREE.

## Results

### Oxygen Isotope in Phosphate ( $\delta^{18}\text{O}_{\text{PO}_4}$ )

The mosasaur tooth samples from Antarctica have an average  $\delta^{18}\text{O}_{\text{PO}_4}$  value of  $19.8 \pm 0.9\%$

for their enamel ( $n = 13$ ) and  $20.9 \pm 1.5\%$  for their dentine ( $n = 6$ ). The two mosasaur teeth from Patagonia have an average  $\delta^{18}\text{O}_{\text{PO}_4}$  value of  $19.2 \pm 0.9\%$  and  $20.6 \pm 0.4\%$  for their enamel and dentine tissues, respectively. Plesiosaur tooth enamel from Antarctica ( $n = 5$ ) have  $\delta^{18}\text{O}_{\text{PO}_4}$  values of  $18.6 \pm 1.6\%$ , while a single dentine sample resulted in a  $\delta^{18}\text{O}_{\text{PO}_4}$  value of  $19.7\%$ . The  $\delta^{18}\text{O}_{\text{PO}_4}$  value of the bony fish tooth enameloid ( $n = 3$ ) from Antarctica is  $23.1 \pm 0.1\%$ , and that of a single dentine sample is  $22.6\%$ . Shark teeth from Patagonia have an average  $\delta^{18}\text{O}_{\text{PO}_4}$  value of  $22.0 \pm 0.4\%$  for their enameloid ( $n = 3$ ) and  $20.7 \pm 1.8\%$  for their dentine ( $n = 2$ ).

#### Oxygen and Carbon Isotope Composition in Structural Carbonate ( $\delta^{18}\text{O}_{\text{CO}_3}$ and $\delta^{13}\text{C}$ )

Mosasaur tooth enamel from Antarctica ( $n = 13$ ) has an average  $\delta^{13}\text{C}$  value of  $-11.3 \pm 2.2\%$  and a  $\delta^{18}\text{O}_{\text{CO}_3}$  value of  $26.9 \pm 0.8\%$ , while dentine ( $n = 14$ ) has a  $\delta^{13}\text{C}$  value of  $-6.0 \pm 2.6\%$  and a  $\delta^{18}\text{O}_{\text{CO}_3}$  value of  $27.5 \pm 0.5\%$ . In one instance (ARG-2), we analyzed associated bone, which has  $\delta^{13}\text{C}_{\text{CO}_3}$  and  $\delta^{18}\text{O}_{\text{CO}_3}$  values of  $-14.0\%$  and  $30.3\%$ , respectively. Two mosasaur tooth enamel samples from Patagonia have respective mean  $\delta^{13}\text{C}_{\text{CO}_3}$  and  $\delta^{18}\text{O}_{\text{CO}_3}$  values of  $-11.1 \pm 0.0\%$  and  $26.1 \pm 0.7\%$ , while the dentine values are  $-3.2 \pm 0.5\%$  and  $26.7 \pm 0.4\%$ , respectively.

The plesiosaur tooth enamel ( $n = 5$ ) from Antarctica yielded an average  $\delta^{13}\text{C}_{\text{CO}_3}$  value of  $-11.8 \pm 0.9\%$  and a  $\delta^{18}\text{O}_{\text{CO}_3}$  value of  $26.9 \pm 1.7\%$ . The plesiosaur dentine ( $n = 5$ ) produced a  $\delta^{13}\text{C}$  value of  $-6.7 \pm 1.1\%$  and a  $\delta^{18}\text{O}_{\text{CO}_3}$  value of  $27.9 \pm 1.1\%$ .

Bony fish tooth enameloid ( $n = 3$ ) from Antarctica has an average  $\delta^{13}\text{C}$  of  $-4.8 \pm 0.6\%$  and  $\delta^{18}\text{O}_{\text{CO}_3}$  of  $29.4 \pm 0.4\%$ , while their dentine ( $n = 3$ ) yielded  $\delta^{13}\text{C}$  and  $\delta^{18}\text{O}_{\text{CO}_3}$  values that averaged  $3.5 \pm 0.9\%$  and  $27.3 \pm 0.2\%$ , respectively.

Finally, shark tooth enameloid ( $n = 4$ ) has an average  $\delta^{13}\text{C}$  value of  $+7.2 \pm 1.8\%$  and a  $\delta^{18}\text{O}_{\text{CO}_3}$  value of  $25.7 \pm 0.3\%$ , while the isotopic values of corresponding dentine ( $n = 4$ ) are  $\delta^{13}\text{C} = -1.1 \pm 0.4\%$  and  $\delta^{18}\text{O}_{\text{CO}_3} = 25.6 \pm 0.2\%$ .

#### Trace Elements Composition

Six tooth specimens from Antarctica (three mosasaurs, two plesiosaurs, and one fish)

and four from Patagonia (one mosasaur and three sharks) were measured for trace element concentrations (see Supplementary Table 1). For Antarctica, the total REE and U content varies between  $1.3$  and  $3553 \mu\text{g/g}$  and  $0.2$  and  $6.1 \mu\text{g/g}$ , respectively, except two remains that had exceptionally high total REE ( $>4000 \mu\text{g/g}$ ): the enameloid of the bony fish (ARG-16) and part of the enamel of a mosasaur tooth (ARG-12A). All other Antarctic samples have REE content lower than  $200 \mu\text{g/g}$ , but it must be mentioned that, in two cases (ARG-1 and ARG-4), the REE content of enamel was too low to obtain a consistent signal. The REE values in the Patagonian samples range from  $27$  to  $6899 \mu\text{g/g}$ , while the U varies between  $0.4$  and  $15.3 \mu\text{g/g}$ . The dentine of the mosasaur tooth (ARG-18) had the highest concentrations in our entire dataset.

A concentration offset between enamel and dentine is evident; however, it is not consistent, and in many cases enamel yielded higher total REE concentration than dentine, especially in the Antarctic sample set. Despite the large variation in REE concentration, the REE distributions within the same specimen fluctuate less, and the majority of the analyses yielded slight MREE enrichment or flat patterns, while others displayed slight HREE enrichment (Fig. 2). The LREE/HREE versus MREE/MREE\* graph expresses variation among the samples. Most of the Antarctic fossils cluster together with a somewhat larger variation in their LREE/HREE ratios than the Patagonian samples, with the exception of the dentine and bone of a single Antarctic specimen (ARG-1 and 2) that plot away from the rest with relatively higher HREE content. In the Patagonian assemblage, the shark teeth and the mosasaur tooth show two discrete clusters, with more HREE enrichment in the shark teeth.

## Discussion

### Preservation of the Isotopic Signature

*Comparison of Isotopic Compositions between Tissues and Ions.*—The pristine state of the original isotopic signature of fossil material cannot be established with certainty (e.g., Kolodny et al. 1996; Fricke and Rogers 2000; Pucéat et al. 2003; Zazzo et al. 2004). However,

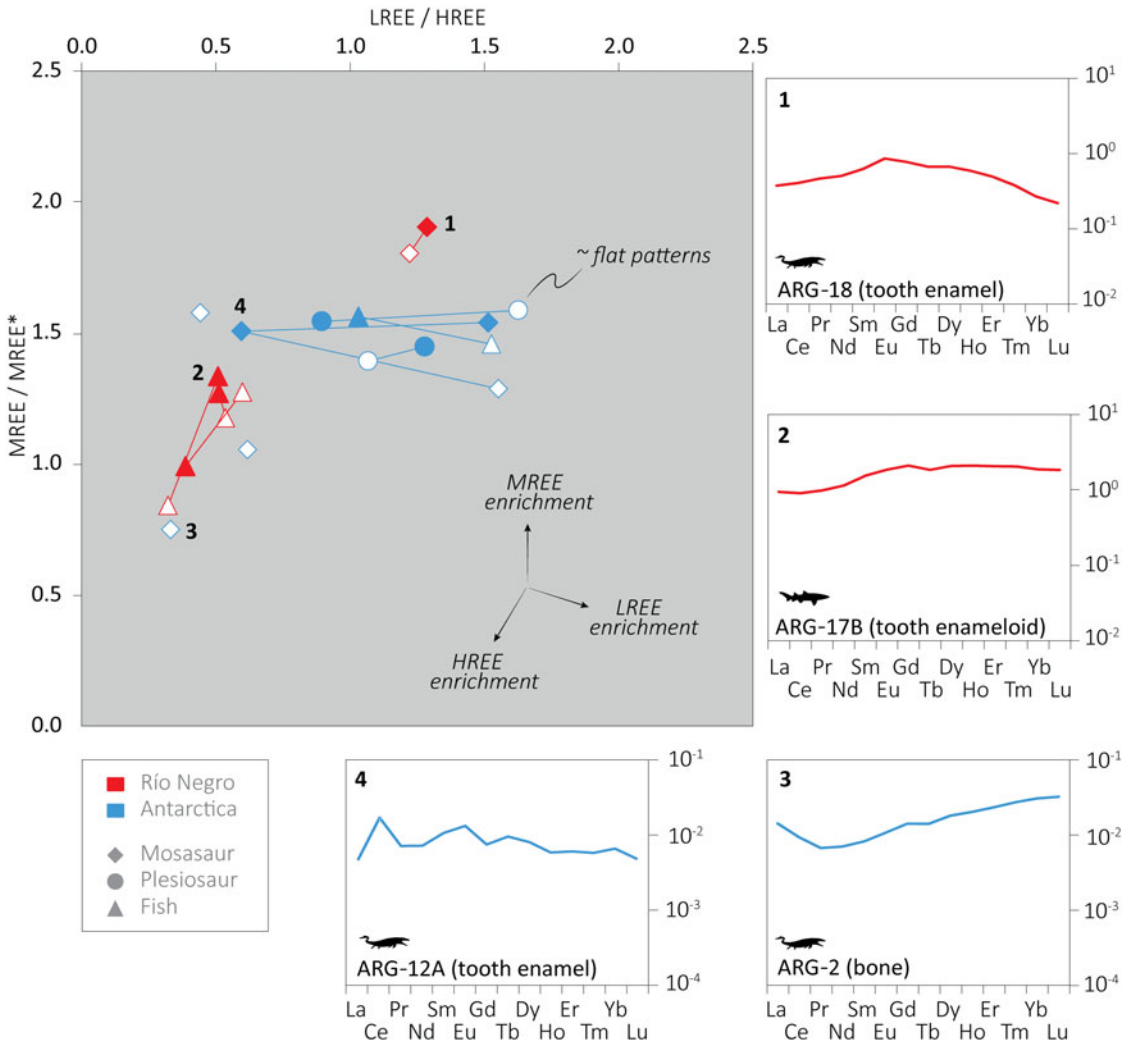


FIGURE 2. Post Archean Australian Shale (PAAS) shale-normalized rare earth element (REE) ratios and REE patterns. Light (LREE) = La, Pr, Ce, Nd; middle (MREE) = Eu, Gd, Tb, Dy; heavy (HREE) = Er, Tm, Yb, Lu; MREE\* = average LREE+HREE; = mosasaur; = shark; open symbols = dentine; solid symbols = enamel(oid).

a good evaluation of the preservation can be achieved in vertebrate remains by comparing the isotopic composition of tissues that react differently to alteration, due to differing microstructure and organic content. Fossils exposed to similar diagenetic conditions should have their densest, most mineralized hard parts (i.e., enamel/enameloid) less altered than more porous tissues such as dentine or bone. In case of an extensive diagenetic alteration, the isotopic composition of all tissues may be homogenized and almost entirely secondary, reflecting the diagenetic fluids rather than the ambient

water or ingested food of the studied organism. A consistent offset between enamel(oid) and dentine or bone in all samples of a single site suggests that at least part of the original signal is preserved in the most resistant fraction (e.g., Zazzo et al. 2004; Amiot et al. 2011; Leuzinger et al. 2015). Such an offset also reveals whether the diagenetic alteration shifts the original isotopic composition toward lower or higher values, which helps to characterize the nature of the diagenetic fluids. For marine organisms, however, early diagenesis is often driven by marine pore fluids that might result in secondary isotopic

values that differ only slightly—if at all—from those of the pristine material.

The phosphate ion is especially resistant to diagenetic alteration, and the  $\delta^{18}\text{O}_{\text{PO}_4}$  values measured in enamel(oid) are particularly suited for paleoenvironmental studies (Iacumin et al. 1996; Zazzo et al. 2004). Regarding the structural carbonate of bioapatite and its isotopic values ( $\delta^{18}\text{O}_{\text{CO}_3}$  and  $\delta^{13}\text{C}$ ) and related ecological applications, the oxygen isotope composition has a lower chance of being preserved compared with carbon. Isotopic exchange is indeed more likely to occur between the oxygen of the diagenetic fluids and the biomineralized tissues, simply because the fluids contain much more oxygen than carbon (Wang and Cerling 1994).

In our results, all enamel(oid)–dentine pairs of single teeth show an offset in both their  $\delta^{18}\text{O}_{\text{PO}_4}$  and  $\delta^{13}\text{C}$  values (Table 1), as well as a clear difference between fish and marine reptiles, which we take as a good sign of enamel preservation. Overall, the enamel  $\delta^{18}\text{O}_{\text{PO}_4}$  values are lower than their dentine counterparts in mosasaurs (by 1.6‰ on average,  $n = 8$ ). This  $^{18}\text{O}$  enrichment of dentine was likely driven by alteration through pore water colder than the reptiles' body temperature, resulting in higher  $\delta^{18}\text{O}_{\text{PO}_4}$  values than the original ones (e.g., Lécuyer et al. 2013). On the other hand, fish teeth result in values higher in enameloid than in dentine (by 1.2‰ on average,  $n = 3$ ); however, in two of the three enameloid–dentine pairs analyzed (ARG-16A and ARG-17C), this difference falls within the standard deviation. This could reflect the fact that marine diagenesis only generates small changes for organisms that have body temperature and body water  $\delta^{18}\text{O}$  values close to those of the ambient water.

As for the carbon isotope composition, there is a clear pattern of the tooth enamel(oid)  $\delta^{13}\text{C}$  values being lower than the dentine counterpart (by 5.6‰ on average in marine reptiles and 8.3‰ in bony fish) in all taxa but sharks, for which the enameloid  $\delta^{13}\text{C}$  values are higher than the dentine values by 8.3‰ on average (Fig. 3A). Especially high  $\delta^{13}\text{C}$  values for shark enameloid have already been observed (e.g., Vennemann et al. 2001; van Baal et al. 2013; Kocsis et al. 2014), but have not yet been entirely explained (see “ $\delta^{13}\text{C}$  Values of Shark

Enameloid: Driven by Biomineralization Rather Than Diet”). In the case of the other taxa, the higher  $\delta^{13}\text{C}$  values in dentine than in enamel(oid) point to a participation of dissolved inorganic carbon (DIC) from the diagenetic fluids that altered the original isotopic signature of the least-resistant tissues (i.e., dentine) and pushed their  $\delta^{13}\text{C}$  values toward more positive values. In the Patagonian material (again, except in sharks), dentine samples are merging toward common  $\delta^{13}\text{C}$  values (−3.6 to −0.7‰) that are likely close to the isotopic composition of the diagenetic fluids. We could not recognize any trend between the  $\delta^{18}\text{O}_{\text{CO}_3}$  values of the different tissues, which suggest a certain degree of alteration.

Finally, the  $\delta^{18}\text{O}$  of extant homeothermic vertebrate bioapatite has been shown to present a systematic difference of 7‰ to 9‰ between its carbonate ( $\delta^{18}\text{O}_{\text{CO}_3}$ ) and phosphate ( $\delta^{18}\text{O}_{\text{PO}_4}$ ) fractions, resulting from a different fractionation factor between water and each of these ions (Bryant et al. 1996; Iacumin et al. 1996) at a constant body temperature. This offset has been repetitively used as a proxy for the preservation of the original isotopic signal (e.g., Zazzo et al. 2004; Lécuyer et al. 2010; Rey et al. 2017). In several instances, our marine reptile data show a smaller  $\delta^{18}\text{O}_{\text{CO}_3\text{-PO}_4}$  offset comprised between 6‰ and 7‰, further supporting a partial alteration of one of the fractions, most probably the carbonate. Unsurprisingly, all fish show a lower  $\delta^{18}\text{O}_{\text{CO}_3\text{-PO}_4}$  offset (down to 3‰), which is expected, given their poikilothermic–ectothermic nature.

#### $\delta^{13}\text{C}$ Values of Shark Enameloid: Driven by Biomineralization Rather Than Diet

Although natural material usually has negative  $\delta^{13}\text{C}$  values (Kelly 2000), positive values of shark enameloid as reported here have readily been observed in other datasets (van Baal et al. 2013; Kocsis et al. 2014). Teeth of extant chondrichthyans also have enameloid with  $\delta^{13}\text{C}$  values typically 6‰ to 8‰ higher than dentine  $\delta^{13}\text{C}$  values (Vennemann et al. 2001); the reason for this is so far unknown. A secondary, diffusional isotopic exchange with ambient water DIC was suggested (Vennemann et al. 2001), which would be stronger in the part of the tooth directly exposed to seawater (i.e.,

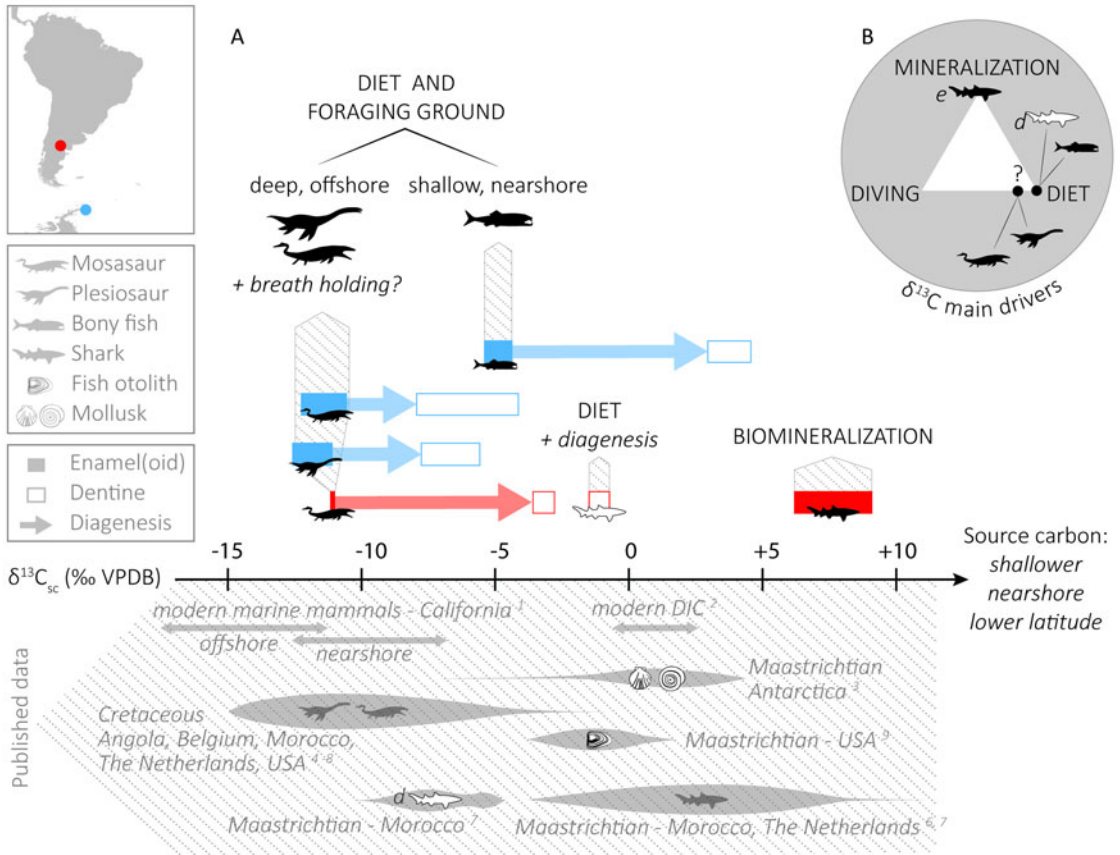


FIGURE 3. A, Top,  $\delta^{13}\text{C}$  ranges for each taxon of this study, and the main parameters that influence their isotopic composition. Diagenetic alteration pushes the  $\delta^{13}\text{C}$  of reptiles and bony fish toward higher values. For sharks, note that unlike dentine, enameloid is not linked to diet, therefore the offset between these tissues is no indicator of diagenetic alteration. Bottom, Literature  $\delta^{13}\text{C}$  data in carbonate from modern and Cretaceous organisms, as well as dissolved inorganic carbon (DIC) values. VPDB, Vienna Pee Dee Belemnite. B, Main drivers of  $\delta^{13}\text{C}$  compositions in pristine material. The “diet” extreme refers to the food source and foraging ground, and hence regroups DIC, latitude, distance from the shore, and depth, whereas “diving” refers to the physiological effect of breath holding. e, enamel(oid); d, dentine. References: 1, Clementz and Koch 2001; 2, Coplen et al. 2002; 3, Tobin and Ward 2015; 4, Robbins et al. 2008; 5, Schulp et al. 2013; 6, van Baal et al. 2013; 7, Kocsis et al. 2014; 8, Strganac et al. 2015; 9, Carpenter et al. 2003.

mostly enameloid). However, some of our shark values are too high (up to 9.8‰) to result from this process alone; indeed, modern DIC in seawater usually does not exceed 3‰ (e.g., Böhm et al. 1996; Coplen et al. 2002; Mackensen and Schmiedl 2019). The mode of enameloid formation in sharks may also play a role via a process of organic matter removal enhanced by enzymes at a late stage of enamel mineralization (Kocsis et al. 2015). A similar enzymatic process has been observed in mammals, with the involvement of the element zinc (e.g., Goettig et al. 2010), and high Zn concentration was also reported in modern shark enameloid

(Kocsis et al. 2015). Such an enzymatic reaction may result in carbon isotope fractionation between the newly formed dental tissue and the removed organic matter. Finally, it is noteworthy that shark tooth dentine and enameloid have different origins (odontoblastic vs. ameloblastic, respectively; Kemp 1985; Vennemann et al. 2001).

Even though the mechanism behind high  $\delta^{13}\text{C}$  shark enameloid values has not yet been fully explained, such values are expected and considered to be a further sign of the good preservation of shark enameloid. Furthermore, alteration is hardly considered to be the trigger

for high  $\delta^{13}\text{C}$  values, because diagenetic fluids and DIC would cause such high original  $\delta^{13}\text{C}$  values to be lowered. Here, we calculated an offset of 18.3‰ between shark and mosasaur enamel(oid) from Río Negro, comparable in magnitude to the value of around 17‰ reported by Schulp et al. (2013). These authors, however, interpreted the shark enameloid  $\delta^{13}\text{C}$  values as a diet indicator, whereas we refrain from doing so. We argue that in the case of sharks, dentine is probably a better diet indicator, if unaltered, than enameloid. This also means that the  $\delta^{13}\text{C}$  offset between these tissues does not strictly reflect the direction of the diagenetic alteration (see Fig. 3A).

#### REE: Complex Diagenetic History

Bioapatite of modern teeth and bones has very low REE and U contents (<10 ng/g); however, fossils are often enriched severalfold (Trueman and Tuross 2002). Therefore, these elements unambiguously represent a diagenetic signal that links to early depositional conditions (e.g., pore fluid chemistry). As these conditions can vary with time and also spatially, REE chemistry of fossil vertebrate remains is often used to assess paleoenvironmental conditions, highlight taphonomic processes, trace reworked specimens, or infer the provenance of specimens of unknown stratigraphic origin (e.g., Elderfield and Pagett 1986; Wright et al. 1987; Trueman and Benton 1997; Lécuyer et al. 2004; Shields and Webb 2004; Trueman et al. 2006; Tütken et al. 2008; Kocsis et al. 2009, 2016; Rogers et al. 2010; Suarez et al. 2010). Ideally, when such applications are targeted, relatively thick bone samples should be tested for fractionation, as a separation of REE due to different diffusion rate related to different ion radii can occur (see Trueman et al. 2011; Herwartz et al. 2013), and a prolonged, late diagenetic overprint might also occur for older remains, which can alter early diagenetic signal (Kocsis et al. 2010; Herwartz et al. 2011; Kowal-Linka et al. 2014).

Generally, higher REE content is expected in the more porous dentine and bone, which also have smaller crystal sizes and originally higher organic content than enamel/enameloid (Trueman and Tuross 2002). Surprisingly, many of

the Antarctic samples show an opposite trend, with some enamel samples being more than 700 or 1200 times more enriched than dentine. In contrast, some samples hardly yielded any REE in their enamel (ARG-1 and ARG-4). Considerable variations in the REE concentrations were also observed within a single sample, as in the mosasaur tooth enamel ARG-12A, with more than 2600  $\mu\text{g/g}$  on one side ( $n=2$ ) and only 51  $\mu\text{g/g}$  on the other ( $n=2$ ) (Supplementary Table 1). These observations indicate a complex diagenetic history in the Antarctic assemblage. Enamel with extremely high REE content compared with dentine may have sheltered the internal part of the teeth. Samples with low REE content in their enamel might have been embedded in rock that quickly cemented, blocking migration of pore fluid. One specimen (fragment with tooth and bone: ARG-1 and ARG-2) was indeed found embedded in strongly cemented sedimentary rock, and the different tissues yielded very low REE content (maximal total REE concentration = 19  $\mu\text{g/g}$ , in dentine), supporting this interpretation. Although we observed some variation in the REE patterns of the Antarctic samples, most of them cluster together, which supports a common diagenetic history with similar REE source in the burial environment (see Fig. 2). The outliers correspond to the remains found embedded in the sedimentary rock (ARG-1 and ARG-2). Interestingly, REE patterns similar to those of these outliers (i.e., with HREE-enrichment) were reported by Patrick et al. (2004, 2007) for mosasaurs thought to have suffered diagenesis in presence of oxic, open-marine water. The generally low REE content and the slight HREE enrichment of these samples may reflect fractionation along the REE series when compared with other patterns from Antarctica (Trueman et al. 2011). A broader study with more samples is necessary to get more insight into the REE chemistry of these Antarctic remains.

Most of the Patagonian samples fit the expected differences between enamel/enameloid and dentine, except one shark tooth for which the enameloid is five times more enriched than the dentine. The REE composition of that tooth might also partially relate to the sheltering effect of enameloid on the

internal part of the tooth. Interestingly, the shark teeth yielded somewhat different REE patterns from the mosasaur tooth (see Fig. 2), which indicates that these remains probably originated from different beds with different REE composition in the burial fluid. The MREE-enriched mosasaur tooth might indicate somewhat lower redox conditions than the shark teeth in their respective depositional beds (e.g., Ounis et al. 2008). Still, the observed differences possibly link to a broader range of variation in REE chemistry within the Jagüel Formation, but the few samples obtained do not allow decipherment of spatial and temporal details.

### $\delta^{13}\text{C}$ , Diet Source, and Feeding Ground

The stable carbon isotope composition of vertebrate bioapatite mainly derives from ingested food (except in chondrichthyan enameloid as detailed in “ $\delta^{13}\text{C}$  Values of Shark Enameloid: Driven by Biomineralization Rather Than Diet”), and it is therefore commonly used to study diet (e.g., DeNiro and Epstein 1978; Hobson and Welch 1992; Bocherens et al. 1994). In the case of marine vertebrate macrofauna, however, the bioapatite carbon isotope composition serves as a general indicator of the source diet rather than giving clues on high-resolution trophic relations as stable calcium isotopes would (Rau et al. 1983; Wada et al. 1987; Fry 1988; Hobson and Welch 1992; Hobson 1993; Hobson et al. 1994; Kelly 2000; Clementz et al. 2003). In marine organisms, the  $\delta^{13}\text{C}$  values ultimately reflect the composition of the DIC or the particulate organic matter (POM) assimilated by the organisms at the very base of the trophic chain, with metabolic effects superimposed.

Both the  $\delta^{13}\text{C}_{\text{DIC}}$  and the  $\delta^{13}\text{C}_{\text{POM}}$  decrease with increasing latitude, distance from the shore, and depth (Fry 1988; Hobson 1993; Goericke and Fry 1994; Hobson et al. 1994; Marchal et al. 1998; Clementz and Koch 2001; Hofmann and Heesch 2018), meaning that the  $\delta^{13}\text{C}$  composition of marine organisms strongly depends on their foraging ground. In our context, we would thus expect a given taxon from the high-paleolatitude site (Antarctica, 64°S) to have lower  $\delta^{13}\text{C}_{\text{CO}_3}$  values than those from the medium-paleolatitude site (Patagonia, 45°S).

Furthermore, anatomic and isotopic evidence suggests that some mosasaur taxa were divers and had deeper foraging grounds (Sheldon 1997; Schulp et al. 2013, 2017; Harrell et al. 2016). A deeper and offshore food source would cause their bioapatite to have lower  $\delta^{13}\text{C}$  values than coexisting shallow-water, nearshore organisms. Clementz and Koch (2001) compared the carbon isotope composition of the tooth apatite of marine mammals from California with different foraging grounds and reported  $\delta^{13}\text{C}$  values between -14‰ and -12‰ for pinnipeds feeding offshore, while nearshore cetaceans had values between -11‰ and -9‰, showing that differences in the foraging ground can induce an offset of ~5‰. Our results show a very clear difference between marine reptiles and bony fish, the former having significantly lower  $\delta^{13}\text{C}$  values (-11.2‰ and -11.8‰ for mosasaurs and plesiosaurs, respectively, compared with -4.8‰ for bony fish), supporting more offshore and/or deeper food sources for reptiles. We obtained similar  $\delta^{13}\text{C}$  values for all mosasaurs and plesiosaurs (average -11.4‰,  $n=20$ ), independent from their latitude of provenance, with the mosasaurs showing a wider scatter, possibly partly explained by a larger and taxonomically more diverse sample set (15 mosasaur samples vs. 5 plesiosaur samples). While the average  $\delta^{13}\text{C}$  composition is similar between mosasaurs from Patagonia (-11.1‰,  $n=2$ ) and Antarctica (-11.3‰,  $n=13$ ), we observed more variation in the Antarctic material (2.2‰ SD), with some samples clearly standing out (ARG-15 = -15.4‰, ARG-10 = -6.8‰). Again, this is most likely driven by the larger sample size and higher taxonomic variety, and hence potentially different feeding habits and ecological niches. However, a limited contribution of dentine in the enamel samples during sampling may also explain the few higher  $\delta^{13}\text{C}$  values when the dentine values are also especially high, as in sample ARG-10 (Fig. 3). The bony fish teeth have clearly higher  $\delta^{13}\text{C}$  compositions (average -4.8‰), suggesting that these fish had a foraging ground shallower and closer to the shore than the marine reptiles. Literature  $\delta^{13}\text{C}$  data are scarce when it comes to the inorganic fraction of Late Cretaceous marine fish

teeth, but a study on Maastrichtian fish otoliths presented isotopic values several per mille higher than those measured in our tooth material (Carpenter et al. 2003; see Fig. 3A). Otoliths are known to reflect the composition of seawater (i.e., DIC; Degens et al. 1969; Patterson 1999), which is isotopically heavier than the dietary carbon source from which other biomineralized tissues such as teeth and bones derive. As a further comparison, shelled mollusks from the same formation and site as our Antarctic material (LBF, Isla Marambio) have on average comparatively  $^{13}\text{C}$ -enriched average values ( $-1.9\text{‰}$  for ammonites and  $+1.9\text{‰}$  for benthic bivalves; Tobin and Ward 2015; see Fig. 3A). Higher values are expected in shells, because their  $\delta^{13}\text{C}$  strongly correlates with that of water DIC (McConnaughey and McRoy 1979; Poulain et al. 2010).

#### Diving Behavior and Isotopic Signature

A deep diving behavior has been proposed for some mosasaurs based on osteological observations (Sheldon 1997; Yamashita et al. 2012) and their low  $\delta^{13}\text{C}$  values compared with non-diving taxa such as sharks (Schulp et al. 2013). A study on extant sea turtles (leatherback and olive ridley turtles; Biasatti 2004) suggests that breath holding during diving could deplete  $^{13}\text{C}$  in body fluids. This depletion would be reflected in low bioapatite  $\delta^{13}\text{C}$  values—closer to the food source composition—in sea turtles that spend a large part of their life diving (dives up to 80 minutes long for the leatherback turtle [López-Mendilaharsu et al. 2009] and up to 200 minutes long for the olive ridley turtle [McMahon et al. 2007]). Although we do not challenge the hypothesis that some mosasaur species were deep divers and hence held their breath for prolonged periods of time, we are cautious regarding the actual driver of their low  $\delta^{13}\text{C}$  values and question whether these are induced by breath holding itself.

Schulp et al. (2013) mainly base their conclusions on a large offset (17‰) between the  $\delta^{13}\text{C}$  values of mosasaur enamel and shark enameloid, which they assume to result from contrasting respiratory physiologies. However, we have already mentioned that shark enameloid is known to have especially high  $\delta^{13}\text{C}$  values

compared with other taxa, a peculiarity likely linked to biomineralization rather than ecology (see discussion in “ $\delta^{13}\text{C}$  Values of Shark Enameloid: Driven by Biomineralization Rather Than Diet”). Because sharks apparently do not record environmental parameters in their tooth enameloid  $\delta^{13}\text{C}$  values, a comparison with mosasaur enamel to draw ecological conclusions is misleading. We also observe a striking difference between mosasaur and shark enamel(oid) (18.4‰) in our material, but interestingly, this offset diminishes dramatically when mosasaurs are compared with another non-diving taxon, namely bony fish (6.4‰). In that case, because enamel(oid) of both bony fish and mosasaur is thought to reflect environmental parameters, part of this offset can be attributed to different respiratory physiologies: dissolved  $\text{CO}_2$  in the water respired by gill-breathing vertebrates is  $^{13}\text{C}$ -enriched compared with atmospheric  $\text{CO}_2$  respired by pulmonate vertebrates (Biasatti 2004), which is reflected in their tissues. However, the largest part of the offset is likely explained by different foraging grounds, as revealed in the previous section; that is, an offshore, deeper food source for mosasaurs than for the bony fish investigated here. Clementz and Koch (2001) indeed reported similarly low  $\delta^{13}\text{C}$  values for two pulmonate and diving taxa, both considered offshore dwellers (northern elephant seal and northern fur seal) but strongly differing in the duration of their dives (up to 2 hours for the former, and in the minute range for the latter; Costa 2007; Kuhn et al. 2010). This suggests that breath holding is not the main driver of low  $\delta^{13}\text{C}$  values, even if it might contribute to them.

To sum up, the food source of diving animals (deeper water, hence isotopically lighter POM and/or DIC reflected in the prey items) is a major driver of their  $\delta^{13}\text{C}$  values, more than the process of breath holding itself, and might well fully explain the low  $\delta^{13}\text{C}$  values measured in plesiosaurs and mosasaurs (Fig. 3B).

$\delta^{18}\text{O}_{\text{PO}_4}$ : Water Temperature, Thermoregulation, and Latitudinal Temperature Gradient

The  $\delta^{18}\text{O}$  values of vertebrate bioapatite depend on the isotopic composition of the body water from which it precipitated, as well

as on the temperature during mineral formation (i.e., body temperature). Two parameters that have a combined effect on the ambient and/or body temperature are (1) the latitude generally representing the distribution of solar heat on the Earth's surface, which could somewhat be modified by oceanic currents in the marine realm; and (2) whether an animal is thermoconformer (i.e., body temperature is linked to external, ambient conditions) or thermoregulator (i.e., using external or internal heat to increase body temperature; Withers 1992). There is strong evidence suggesting that mosasaurs and plesiosaurs could produce metabolic heat (endothermy) and maintain a constant body temperature (homeothermy) independent from the ambient temperature, and thus from the latitude at which they lived (Bernard et al. 2010; Harrell et al. 2016). For these taxa, variations in the  $\delta^{18}\text{O}_{\text{PO}_4}$  values between samples from different paleolatitudes should thus be limited to—and mainly driven by—the  $\delta^{18}\text{O}_{\text{body water}}$  values, which can vary with the isotopic composition of the ambient water, as well as with physiological processes that can respond to body mass (e.g., Tejada-Lara et al. 2018; Villamarín et al. 2018). In contrast, both the  $\delta^{18}\text{O}_{\text{body water}}$  values and the body temperature of aquatic, thermoconforming animals (e.g., ectotherms) such as most fish are similar to that of the surrounding water, meaning that their  $\delta^{18}\text{O}_{\text{PO}_4}$  values are closely related to latitudinal thermal variations. Fish bioapatite mineralizes in isotopic equilibrium with the ambient water, and according to water–phosphate fractionation equations (Kolodny et al. 1983; Lécuyer et al. 2013),  $\delta^{18}\text{O}_{\text{PO}_4}$  values increase with decreasing precipitation temperature. The assumption of high-latitude Antarctic fish  $\delta^{18}\text{O}_{\text{PO}_4}$  values being higher than those of Patagonian fish is supported by our data ( $\Delta^{18}\text{O}_{\text{Ant-Pat}} = 1.1\text{‰}$ ; Fig. 4).

Meanwhile, the  $\delta^{18}\text{O}_{\text{PO}_4}$  values of homeothermic–endothermic marine reptiles are more stable across latitudes, as expected. Additionally, the ambient water temperature at our study sites was most likely lower than mosasaur and plesiosaur body temperatures (e.g., Bernard et al. 2010), which is reflected in reptiles'  $\delta^{18}\text{O}_{\text{PO}_4}$  values being overall lower than those of fish (Fig. 4).

An estimation of the water temperature can be derived from fish  $\delta^{18}\text{O}_{\text{PO}_4}$  values using the Lécuyer et al. (2013) fractionation equation defined as:

$$T = 117.4 - 4.5 * (\delta^{18}\text{O}_{\text{PO}_4} - \delta^{18}\text{O}_{\text{water}}) \quad (1)$$

where  $T$  is the temperature in degrees Celsius and  $\delta$  is expressed in ‰ against the VSMOW scale.

Considering a global  $\delta^{18}\text{O}_{\text{seawater}}$  of  $-1.25\text{‰}$  (as in Pucéat et al. [2007], for the sake of comparison), that is, lower than today's average due to the absence of a permanent ice cap during the Late Cretaceous (Shackleton and Kennett 1976), our fish enameloid material results in a water temperature of  $12.7 \pm 1.9^\circ\text{C}$  for the Patagonian site ( $45^\circ\text{S}$ ) and  $7.9 \pm 0.5^\circ\text{C}$  for the Antarctic ( $64^\circ\text{S}$ ) site. In Figure 4, we have plotted published water temperatures derived from fish  $\delta^{18}\text{O}_{\text{PO}_4}$ , with a latitudinal correction of the  $\delta^{18}\text{O}_{\text{water}}$  following Zachos et al. (1994: Supplementary Table 2). For our material, we obtain slightly different temperatures after that correction:  $13.7^\circ\text{C}$  and  $6.8^\circ\text{C}$  for our Patagonian and Antarctic sites, respectively (see Fig. 4).

When compared with published values, higher temperatures have been reported by some authors for  $40^\circ$ – $50^\circ$  paleolatitudes based on fish bioapatite  $\delta^{18}\text{O}_{\text{PO}_4}$  (e.g., Pucéat et al. 2007) and other proxies such as  $\text{TEX}_{86}$  (Woelders et al. 2017). On the other hand, our Patagonian data follow a latitudinal trend when compared with other fish  $\delta^{18}\text{O}_{\text{PO}_4}$  data from slightly higher paleolatitudes (Fig. 4). Regarding our Antarctic water temperatures, they are fall within the  $\sim 5^\circ\text{C}$ – $14^\circ\text{C}$  range calculated based on  $\delta^{18}\text{O}$  values for Maastrichtian cephalopods and shelled mollusks from the same area as our material, adjusted to a  $\delta^{18}\text{O}_{\text{seawater}}$  of  $-1.25\text{‰}$  (Ditchfield et al. 1994; Li and Keller 1999; Dutton et al. 2007; Tobin et al. 2012; Woelders et al. 2017). To our knowledge, no other water temperatures have been reported for high latitudes based on fish  $\delta^{18}\text{O}_{\text{PO}_4}$ .

As for the body temperature of marine reptiles, the water–phosphate fractionation equation (eq. 1) cannot be directly transferred to endotherms, because it was defined for thermoconforming organisms, and unknown

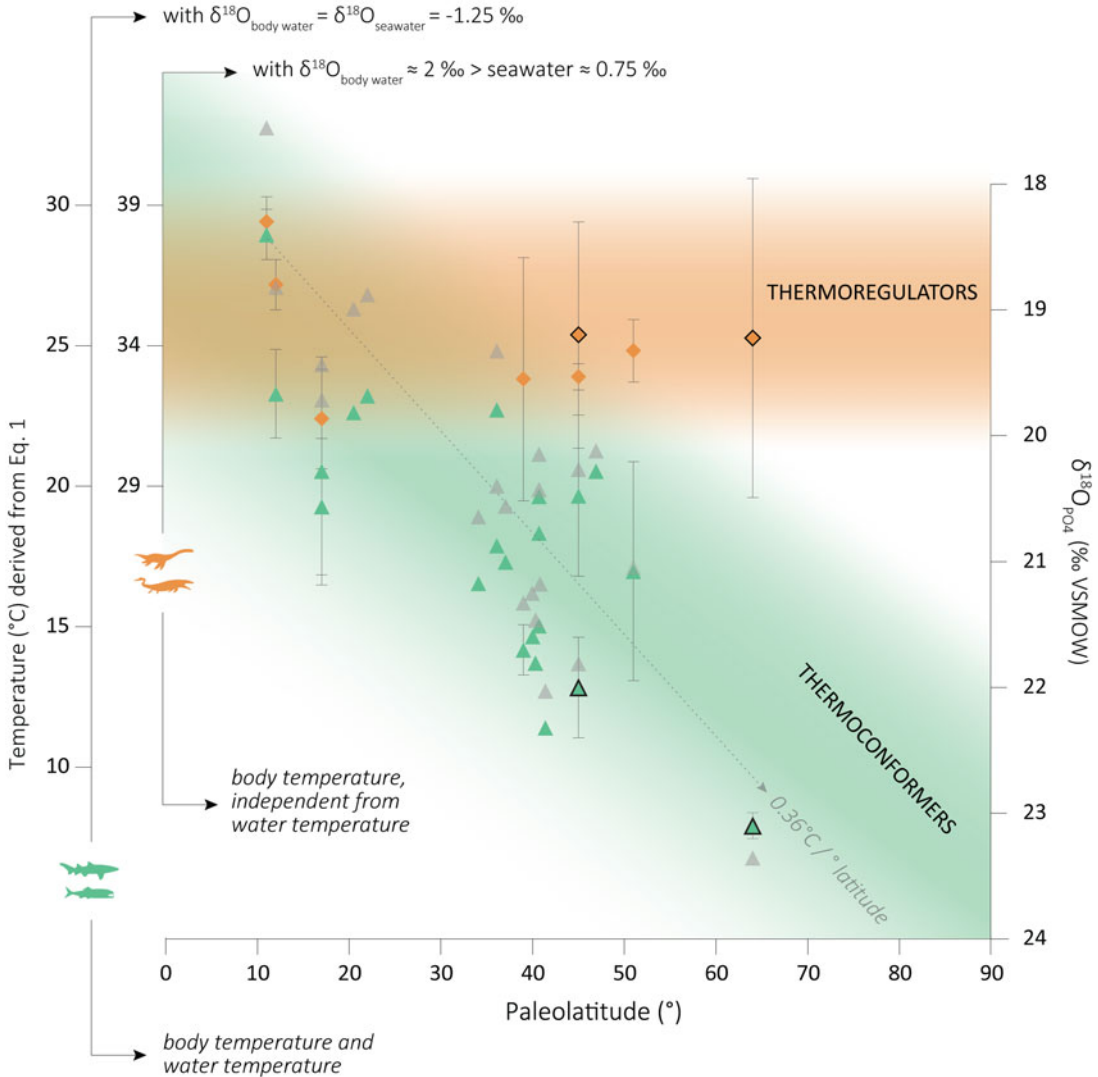


FIGURE 4. Paleolatitudinal distribution of Campanian–Maastrichtian marine vertebrate  $\delta^{18}\text{O}_{\text{PO}_4}$  data from this study (colored closed symbols) and from the literature (colored open symbols), and respective body temperature according to eq. 1, using different  $\delta^{18}\text{O}_{\text{water}}$  values (see main text). Green symbols: thermoconforming bony fish and sharks; orange symbols: thermoregulating mosasaurs and plesiosaurs; gray symbols: water temperatures derived from fish  $\delta^{18}\text{O}_{\text{PO}_4}$  values after a latitudinal correction of  $\delta^{18}\text{O}_{\text{seawater}}$  following Zachos et al. (1994), and resulting thermal gradient. Note that the gray data points do not correlate with the  $\delta^{18}\text{O}_{\text{PO}_4}$  y-axis, because the latitudinal adjustment is nonlinear. Literature data from Puc at et al. (2007), Bernard et al. (2010), and Kocsis et al. (2014). VSMOW, Vienna Standard Mean Ocean Water.

and/or unquantified vital effects might drive the biapatite mineralization out of equilibrium. Nevertheless, some authors (e.g., S on et al. 2020) have used it as an approximation for marine reptile body temperature, considering an  $^{18}\text{O}$  enrichment of about 2‰ of the  $\delta^{18}\text{O}_{\text{body water}}$  relative to ambient water, that is, similar to that observed in extant aquatic

pulmonate vertebrates (see Bernard et al. 2010). Using the same criteria, we obtain elevated body temperatures (roughly between 30°C and 40°C) for both our middle- and high-latitude reptiles (Fig. 4). We do not aim here to define the absolute body temperatures of mosasaurs and plesiosaurs, but these estimates illustrate well the order of magnitude in terms

of body temperature differences between thermoconformers and thermoregulators (here endotherms) with increasing latitude.

These new high-latitude  $\delta^{18}\text{O}_{\text{PO}_4}$  values add a missing piece to the latitudinal gradient of fish bioapatite for the Cretaceous, which so far did not exceed 52° paleolatitude (Pucéat et al. 2007; Bernard et al. 2010). Zhang et al. (2019) proposed a global gradient of 0.41°C/1° of latitude for the latest Cretaceous based on  $\delta^{18}\text{O}_{\text{PO}_4}$  values of fish remains (otoliths and teeth) and foraminifera, as well as the  $\text{TEX}_{86}$  paleotemperature proxy, after correcting for different biases such as latitude and seasonality. These authors highlighted two points of inflection on their latitudinal gradient (at 35° and 52°, respectively), resulting in a steeper middle-latitude gradient and comparatively shallower low- and high-latitude gradients. These changes in the gradient slope are interpreted as reflecting the formation of subtropical and polar fronts and an evolution toward a more stratified ocean. Based on  $\delta^{18}\text{O}_{\text{PO}_4}$  fish data, Pucéat et al. (2007) described the latest Cretaceous marine gradient as globally similar to the present gradient (around 0.4°C/1° of latitude) between 10° and 50° paleolatitude. These authors apply a latitudinal adjustment of the  $\delta^{18}\text{O}_{\text{seawater}}$  following the correction of Zachos et al. (1994) established for Cenozoic times between 0° and 70° latitude. This nonlinear correction results in changes in the gradient slope similar to the model of Zhang et al. (2019), that is, a steeper slope at the middle portion. Applying the same latitudinal correction to our data, we obtain a similar latitudinal gradient of 0.36°C/1° of latitude (Fig. 4).

The combination of our new high-latitude fish  $\delta^{18}\text{O}_{\text{PO}_4}$  values with the Campanian–Maastrichtian literature fish data supports the global gradients established to date (around 0.4°C/1° of latitude). This reiterates the potential of fish bioapatite as a paleotemperature proxy as reliable as foraminifers and bivalves. This global gradient possibly reflects the combination of shallower low- and high-latitude gradients with a steeper middle-latitude gradient as proposed by Zhang et al. (2019) and already suggested by Pucéat et al. (2007). The water temperatures (around 8°C) calculated from our fish  $\delta^{18}\text{O}_{\text{PO}_4}$  values for a 64° paleolatitude

are slightly above modern sea-surface temperatures for similar latitude (LEVITUS 1994), even considering the entire range of seasonal variations, which aligns well with the model of a world devoid of long-lasting ice caps on the poles during the latest Maastrichtian. As for marine reptiles, the highest paleolatitude  $\delta^{18}\text{O}_{\text{PO}_4}$  data published to date came from 52° S (Australia; Bernard et al. 2010). These new mosasaur and plesiosaur high-latitude values further support endothermic and probably also homeothermic thermoregulation and relatively stable  $\delta^{18}\text{O}_{\text{PO}_4}$  values across latitudes and allow us to considerably extend the current database for marine reptiles by 12° to the south.

## Conclusions

The fossil material analyzed here shows well-preserved  $\delta^{13}\text{C}$  and  $\delta^{18}\text{O}_{\text{PO}_4}$  values that reflect differences between taxa in their ecology and/or latitudinal provenance. Marine reptile (mosasaurs and plesiosaurs)  $\delta^{13}\text{C}$  values suggest deeper, more-offshore foraging grounds than associated fish. We suggest that an offshore, deep,  $^{13}\text{C}$ -depleted food source is the main driver of their globally low  $\delta^{13}\text{C}$  values and that a major influence of breath holding on isotopic fractionation related to diving, as previously proposed, is secondary. We also emphasize that  $\delta^{13}\text{C}$  values of shark enameloid should not be compared with those of other taxa in ecological studies, as they are most likely unrelated to diet or behavior.

The  $\delta^{18}\text{O}_{\text{PO}_4}$  values of marine reptiles do not correlate with paleolatitude, suggesting an elevated body temperature (i.e., thermoregulation), whereas coexisting bony fish and sharks show expected latitudinal variations in their  $\delta^{18}\text{O}_{\text{PO}_4}$ . Based on fish  $\delta^{18}\text{O}_{\text{PO}_4}$ , we could calculate a seawater temperature around 7°C at 64°S during the latest Maastrichtian, just before the K/Pg extinction event; that is, slightly above present-day values for similar latitudes worldwide and consistent with a world devoid of permanent polar ice caps. These new high-latitude  $\delta^{18}\text{O}_{\text{PO}_4}$  values add an important missing piece to the global database of marine vertebrate bioapatite, so far limited to 52° paleolatitude. The high-latitude fish  $\delta^{18}\text{O}_{\text{PO}_4}$  values in particular further support a latitudinal gradient around

0.4°C/1° of latitude for the latest Cretaceous as published elsewhere based on fish bioapatite, bivalves, and foraminifera.

### Acknowledgments

Partial financial support for this study was provided by the Agencia Nacional de Investigaciones Científicas y Tecnológicas ANPCyT-PICT-2016-1039. Thank you to M. Reguero (Museo de La Plata, Argentina) and D. Cabaza (Museo de Lamarque, Argentina) for the authorization to use fossil samples, and to the Instituto Antártido Argentino (IAA) for logistic support during field trips to Antarctica. We are grateful for the constructive comments of A. Schulp and an anonymous review that helped improving our work.

### Data Availability Statement

Data available from the FigShare Digital Repository: <https://doi.org/10.6084/m9.figshare.21340176>.

### Literature Cited

- Amiot, R., C. Lécuyer, É. Buffetaut, F. Fluteau, S. Legendre, and F. Martineau. 2004. Latitudinal temperature gradient during the Cretaceous Upper Campanian-Middle Maastrichtian:  $\delta^{18}\text{O}$  record of continental vertebrates. *Earth and Planetary Science Letters* 226:255–272.
- Amiot, R., X. Wang, Z. Zhou, X. Wang, É. Buffetaut, C. Lécuyer, Z. Ding, F. Fluteau, T. Hibino, N. Kusuhashi, J. Mo, V. Suteethorn, Y. Wang, X. Xu, and F. Zhang. 2011. Oxygen isotopes of East Asian dinosaurs reveal exceptionally cold Early Cretaceous climates. *Proceedings of the National Academy of Sciences USA* 108:5179–5183.
- Baal, R. R. van, R. Janssen, H. J. L. van der Lubbe, A. S. Schulp, J. W. M. Jagt, and H. B. Vonhof. 2013. Oxygen and carbon stable isotope records of marine vertebrates from the type Maastrichtian, The Netherlands and northeast Belgium (Late Cretaceous). *Palaeogeography, Palaeoclimatology, Palaeoecology* 392:71–78.
- Bernard, A., C. Lécuyer, P. Vincent, R. Amiot, N. Bardet, É. Buffetaut, G. Cuny, F. Fourel, F. Martineau, J.-M. Mazin, and A. Prieur. 2010. Regulation of body temperature by some Mesozoic marine reptiles. *Science* 328:1379–1382.
- Biasatti, D. M. 2004. Stable carbon isotopic profiles of sea turtle humeri: implications for ecology and physiology. *Palaeogeography, Palaeoclimatology, Palaeoecology* 206:203–216.
- Bocherens, H., M. Fizet, and A. Mariotti. 1994. Diet, physiology and ecology of fossil mammals as inferred from stable carbon and nitrogen isotope biogeochemistry: implications for Pleistocene bears. *Palaeogeography, Palaeoclimatology, Palaeoecology* 107:213–225.
- Böhm, F., M. M. Joachimski, H. Lehnert, G. Morgenroth, W. Kretschmer, J. Vacelet, and W. C. Dullo. 1996. Carbon isotope records from extant Caribbean and South Pacific sponges: evolution of  $\delta^{13}\text{C}$  in surface water DIC. *Earth and Planetary Science Letters* 139:291–303.
- Bryant, D. J., P. L. Koch, P. N. Froelich, W. J. Showers, and B. J. Genna. 1996. Oxygen isotope partitioning between phosphate and carbonate in mammalian apatite. *Geochimica et Cosmochimica Acta* 60:5145–5148.
- Carpenter, S. J., J. M. Erickson, and F. D. Holland. 2003. Migration of a Late Cretaceous fish. *Nature* 423:70–74.
- Clemenz, M. T., and P. L. Koch. 2001. Differentiating aquatic mammal habitat and foraging ecology with stable isotopes in tooth enamel. *Oecologia* 129:461–472.
- Clemenz, M. T., P. Holden, and P. L. Koch. 2003. Are calcium isotopes a reliable monitor of trophic level in marine settings? *International Journal of Osteoarchaeology* 13:29–36.
- Coplen, T. B., J. A. Hopple, J. K. Böhlke, H. S. Peiser, S. E. Rieder, H. R. Krouse, K. J. R. Rosman, R. D. Vocke, K. M. Révész, A. Lamberty, P. Taylor, and P. De Bièvre. 2002. Compilation of minimum and maximum isotope ratios of selected elements in naturally occurring terrestrial materials and reagents. U.S. Geological Survey, Water-Resources Investigations Report 01-4222. Reston, Va.
- Costa, D. P. 2007. Diving physiology of marine vertebrates. *In* *Encyclopedia of life sciences*. doi: 10.1002/9780470015902.a0004230.
- Degens, E. T., W. G. Deuser, and R. L. Haedrich. 1969. Molecular structure and composition of fish otoliths. *Marine Biology* 2:105–113.
- DeNiro, M. J., and S. Epstein. 1978. Influence of diet on the distribution of carbon isotopes in animals. *Geochimica et Cosmochimica Acta* 42:495–506.
- Ditchfield, P. W., J. D. Marshall, and D. Pirrie. 1994. High latitude palaeotemperature variation: new data from the Tithonian to Eocene of James Ross Island, Antarctica. *Palaeogeography, Palaeoclimatology, Palaeoecology* 107:79–101.
- Dutton, A., B. T. Huber, K. C. Lohmann, and W. J. Zinsmeister. 2007. High-resolution stable isotope profiles of a dimitobelid belemnite: implications for paleodepth habitat and late Maastrichtian climate seasonality. *Palaios* 22:642–650.
- Elderfield, H., and R. Pagett. 1986. Rare earth elements in ichthyoliths: variations with redox conditions and depositional environment. *Science of the Total Environment* 49:175–197.
- Elliot, D. H., R. A. Askin, F. T. Kyte, and W. J. Zinsmeister. 1994. Iridium and dinocysts at the Cretaceous–Tertiary boundary on Seymour Island, Antarctica: implications for the K-T event. *Geology* 22:675–678.
- Fernández, M. S., and Z. Gasparini. 2012. Campanian and Maastrichtian mosasaurs from Antarctic Peninsula and Patagonia, Argentina. *Bulletin de la Société Géologique de France* 183:93e102.
- Fernández, M., J. Martin, and S. Casadio. 2008. Mosasaurs (Reptilia) from the late Maastrichtian (Late Cretaceous) of northern Patagonia (Río Negro, Argentina). *Journal of South American Earth Sciences* 25:176–186.
- Fricke, H. C., and R. R. Rogers. 2000. Multiple taxon—multiple locality approach to providing oxygen isotope evidence for warm-blooded theropod dinosaurs. *Geology* 28:799–802.
- Fry, B. 1988. Food web structure on Georges Bank from stable C, N, and S isotopic compositions. *Limnology and Oceanography* 33:1182–1190.
- Gasparini, Z., S. Casadio, M. Fernández, and L. Salgado. 2001. Marine reptiles from the Late Cretaceous of northern Patagonia. *Journal of South American Earth Sciences* 14:51–60.
- Gasparini, Z., L. Salgado, and S. Casadio. 2003. Maastrichtian plesiosaurs from northern Patagonia. *Cretaceous Research* 24:157–170.
- Goericke, R., and B. Fry. 1994. Variations of marine plankton  $\delta^{13}\text{C}$  with latitude, temperature, and dissolved  $\text{CO}_2$  in the world ocean. *Global Biogeochemical Cycles* 8:85–90.
- Goettig, P., V. Magdolen, and H. Brandstetter. 2010. Natural and synthetic inhibitors of kallikrein-related peptidases (KLKs). *Biochimie* 92:1546–1567.

- González Ruiz, P., M. S. Fernández, M. Talevi, J. M. Leardi, and M. A. Reguero. 2019. A new *Plotosaurini* mosasaur skull from the upper Maastrichtian of Antarctica. *Plotosaurini paleogeographic occurrences*. *Cretaceous Research* 103:104166.
- Günther, D., R. Frischknecht, C. A. Heinrich, and H.-J. Kahlert. 1997. Capabilities of an argon fluoride 193 nm excimer laser for laser ablation inductively coupled plasma mass spectrometry microanalysis of geological materials. *Journal of Analytical Atomic Spectrometry* 12:939–944.
- Harrell, T. L., Jr., A. Pérez-Huerta, and C. A. Suarez. 2016. Endothermic mosasaurs? Possible thermoregulation of Late Cretaceous mosasaurs (Reptilia, Squamata) indicated by stable oxygen isotopes in fossil bioapatite in comparison with coeval marine fish and pelagic seabirds. *Palaeontology* 59:351–363.
- Herwartz, D., T. Tütken, C. Münker, K. P. Jochum, B. Stoll, and P. M. Sander. 2011. Timescales and mechanisms of REE and Hf uptake in fossil bones. *Geochimica et Cosmochimica Acta* 75:82–105.
- Herwartz, D., T. Tütken, K. P. Jochum, and P. M. Sander. 2013. Rare earth element systematics of fossil bone revealed by LA-ICPMS analysis. *Geochimica et Cosmochimica Acta* 103:161–183.
- Hinsbergen, D. J. J. van, L. V. de Groot, S. J. van Schaik, W. Spakman, P. K. Bijl, A. Sluijs, C. G. Langereis, and H. Brinkhuis. 2015. A paleolatitude calculator for paleoclimate studies. *PLoS ONE* 10:1–21.
- Hobson, K. A. 1993. Trophic relationships among high Arctic seabirds: insights from tissue-dependent stable-isotope models. *Marine Ecology Progress Series* 95:7–18.
- Hobson, K. A., and H. E. Welch. 1992. Determination of trophic relationships within a high Arctic marine food web using  $\delta^{13}\text{C}$  and  $\delta^{15}\text{N}$  analysis. *Marine Ecology Progress Series* 84:9–18.
- Hobson, K. A., J. F. Piatt, and J. Pitocchelli. 1994. Using stable isotopes to determine seabird trophic relationships. *Journal of Animal Ecology* 63:786–798.
- Hofmann, L. C., and S. Heesch. 2018. Latitudinal trends in stable isotope signatures and carbon-concentrating mechanisms of northeast Atlantic rhodoliths. *Biogeosciences* 15:6139–6149.
- Iacumin, P., H. Bocherens, A. Mariotti, and A. Longinelli. 1996. Oxygen isotope analyses of co-existing carbonate and phosphate in biogenic apatite: a way to monitor diagenetic alteration of bone phosphate? *Earth and Planetary Science Letters* 142:1–6.
- Kelly, J. F. 2000. Stable isotopes of carbon and nitrogen in the study of avian and mammalian trophic ecology. *Canadian Journal of Zoology* 78:1–27.
- Kemp, N. E. 1985. Ameloblastic secretion and calcification of the enamel layer in shark teeth. *Journal of Morphology* 184:215–230.
- Koch, P. L., N. Tuross, and M. L. Fogel. 1997. The effects of sample treatment and diagenesis on the isotopic integrity of carbonate in biogenic hydroxylapatite. *Journal of Archaeological Science* 24:417–429.
- Kocsis, L. 2011. Geochemical compositions of marine fossils as proxies for reconstructing ancient environmental conditions. *Chimia* 65:787–791.
- Kocsis, L., A. Ósi, T. W. Vennemann, C. N. Trueman, and M. R. Palmer. 2009. Geochemical study of vertebrate fossils from the Upper Cretaceous (Santonian) Csehbánya Formation (Hungary): evidence for a freshwater habitat of mosasaurs and pycnodont fish. *Palaeogeography, Palaeoclimatology, Palaeoecology* 280:532–542.
- Kocsis, L., C. N. Trueman, and M. R. Palmer. 2010. Protracted diagenetic alteration of REE contents in fossil bioapatites: direct evidence from Lu-Hf isotope systematics. *Geochimica et Cosmochimica Acta* 74:6077–6092.
- Kocsis, L., E. Gheerbrant, M. Mouflih, H. Cappetta, J. Yans, and M. Amaghaz. 2014. Comprehensive stable isotope investigation of marine biogenic apatite from the late Cretaceous–early Eocene phosphate series of Morocco. *Palaeogeography, Palaeoclimatology, Palaeoecology* 394:74–88.
- Kocsis, L., T. W. Vennemann, A. Ulianov, and J. M. Brunnschweiler. 2015. Characterizing the bull shark *Carcharhinus leucas* habitat in Fiji by the chemical and isotopic compositions of their teeth. *Environmental Biology of Fishes* 98:1609–1622.
- Kocsis, L., E. Gheerbrant, M. Mouflih, H. Cappetta, A. Ulianov, M. Chiaradia, and N. Bardet. 2016. Gradual changes in upwelled seawater conditions (redox, pH) from the late Cretaceous through early Paleogene at the northwest coast of Africa: negative Ce anomaly trend recorded in fossil bio-apatite. *Chemical Geology* 421:44–54.
- Kolodny, Y., B. Luz, and O. Navon. 1983. Oxygen isotope variations in phosphate of biogenic apatites: fish bone apatite—rechecking the rules of the game. *Earth and Planetary Science Letters* 64:398–404.
- Kolodny, Y., B. Luz, M. Sander, and W. A. Clemens. 1996. Dinosaur bones: fossils or pseudomorphs? The pitfalls of physiology reconstruction from apatitic fossils. *Palaeogeography, Palaeoclimatology, Palaeoecology*, 126:161–171.
- Kowal-Linka, M., K. P. Jochum, and D. Surmik. 2014. LA-ICP-MS analysis of rare earth elements in marine reptile bones from the Middle Triassic bonebed (Upper Silesia, S Poland): impact of long-lasting diagenesis, and factors controlling the uptake. *Chemical Geology* 363:213–228.
- Kuhn, C. E., Y. Tremblay, R. R. Ream, and T. S. Gelatt. 2010. Coupling GPS tracking with dive behavior to examine the relationship between foraging strategy and fine-scale movements of northern fur seals. *Endangered Species Research* 12:125–139.
- Lécuyer, C., B. Reynard, and P. Grandjean. 2004. Rare earth element evolution of Phanerozoic seawater recorded in biogenic apatites. *Chemical Geology* 204:63–102.
- Lécuyer, C., V. Balter, F. Martineau, F. Fourel, A. Bernard, R. Amiot, V. Gardien, O. Otero, S. Legendre, G. Panczer, L. Simon, and R. Martini. 2010. Oxygen isotope fractionation between apatite-bound carbonate and water determined from controlled experiments with synthetic apatites precipitated at 10–37°C. *Geochimica et Cosmochimica Acta* 74:2072–2081.
- Lécuyer, C., R. Amiot, A. Touzeau, and J. Trotter. 2013. Calibration of the phosphate  $\delta^{18}\text{O}$  thermometer with carbonate–water oxygen isotope fractionation equations. *Chemical Geology* 347:217–226.
- Leuzinger, L., L. Kocsis, J.-P. Billon-Bruyat, S. Spezzaferri, and T. W. Vennemann. 2015. Stable isotope study of a new chondrichthyan fauna (Kimmeridgian, Porrentruy, Swiss Jura): an unusual freshwater-influenced isotopic composition for the hybodont shark *Asteracanthus*. *Biogeosciences* 12:6945–6954.
- LEVITUS. 1994. LEVITUS94, World ocean atlas. <http://ingrid.ideo.columbia.edu/SOURCES/LEVITUS94>, accessed 12 January 2021.
- Li, L., and G. Keller. 1998. Abrupt deep-sea warming at the end of the Cretaceous. *Geology* 26:995–998.
- Li, L., and G. Keller. 1999. Variability in Late Cretaceous climate and deep waters: evidence from stable isotopes. *Marine Geology* 161:171–190.
- Lindgren, J., and M. Siverson. 2005. *Halisaurus Sternbergi*, a small mosasaur with an intercontinental distribution. *Journal of Paleontology* 79:763–773.
- Linnert, C., S. A. Robinson, J. A. Lees, P. R. Bown, I. Pérez-Rodríguez, M. R. Petrizzo, F. Falzoni, K. Littler, J. A. Arz, and E. E. Russell. 2014. Evidence for global cooling in the Late Cretaceous. *Nature Communications* 5:1–7.
- López-Mendilaharsu, M., C. F. D. Rocha, A. Domingo, B. P. Wallace, and P. Miller. 2009. Prolonged, deep dives by the leatherback turtle *Dermochelys coriacea*: pushing their aerobic dive limits. *Marine Biodiversity Records* 200:6–8.
- Macellari, C. E. 1988. Stratigraphy, sedimentology, and paleoecology of Upper Cretaceous/Paleocene shelf-deltaic sediments of Seymour Island. *Geological Society of America Memoir* 169:25–53.

- Mackensen, A., and G. Schmiedl. 2019. Stable carbon isotopes in paleoceanography: atmosphere, oceans, and sediments. *Earth-Science Reviews* 197:102893.
- Marchal, O., T. F. Stocker, and F. Joos. 1998. A latitude-depth, circulation-biogeochemical ocean model for paleoclimate studies. Development and sensitivities. *Tellus* 50B:290–316.
- McConnaughey, T., and C. P. McRoy. 1979. Food-web structure and the fractionation of carbon isotopes in the Bering Sea. *Marine Biology* 53:257–262.
- McMahon, C. R., C. J. A. Bradshaw, and G. C. Hays. 2007. Satellite tracking reveals unusual diving characteristics for a marine reptile, the olive ridley turtle *Lepidochelys olivacea*. *Marine Ecology Progress Series* 329:239–252.
- Montes, M., F. Nozal, S. Santillana, S. Marensi, and E. Olivero. 2007. Mapa geológico de la Isla Marambio (Seymour). Instituto Geológico y Minero de España, Madrid.
- Motani, R. 2010. Warm-blooded “sea dragons”? *Science* 328:1361–1363.
- O’Gorman, J. P., Z. Gasparini, and L. Salgado. 2014. Reappraisal of *Tuarangisaurus? cabazai* (Elasmosauridae, Plesiosauria) from the Upper Maastrichtian of northern Patagonia, Argentina. *Cretaceous Research* 47:39–47.
- O’Gorman, J. P., P. Bona, M. de los Reyes, M. E. Raffi, and M. Reguero. 2020. A non-aristonectine plesiosaur from Antarctica reveals new data on the mandibular symphysis of elasmosaurids. *Alcheringa: An Australasian Journal of Palaeontology* 44:565–576.
- Olivero, E. B. 2012. Sedimentary cycles, ammonite diversity and palaeoenvironmental changes in the Upper Cretaceous Marambio Group, Antarctica. *Cretaceous Research* 34:348–366.
- O’Neil, J. R., L. J. Roe, E. Reinhard, and R. E. Blake. 1994. A rapid and precise method of oxygen isotope analysis of biogenic phosphate. *Israel Journal of Earth Sciences* 43:203–212.
- Unis, A., L. Kocsis, F. Chaabani, and H. R. Pfeifer. 2008. Rare earth elements and stable isotope geochemistry ( $\delta^{13}\text{C}$  and  $\delta^{18}\text{O}$ ) of phosphorite deposits in the Gafsa Basin, Tunisia. *Palaeogeography, Palaeoclimatology, Palaeoecology* 268:1–18.
- Patrick, D., J. E. Martin, D. C. Parris, and D. E. Grandstaff. 2004. Paleoenvironmental interpretations of rare earth element signatures in mosasaurs (Reptilia) from the upper Cretaceous Pierre Shale, central South Dakota, USA. *Palaeogeography, Palaeoclimatology, Palaeoecology* 212(3–4):277–294.
- Patrick, D., J. E. Martin, D. C. Parris, and D. E. Grandstaff. 2007. Rare earth element (REE) analysis of fossil vertebrates from the Upper Cretaceous Pierre Shale Group for the purposes of paleobathymetric interpretations of the Western Interior Seaway. *In* J. E. Martin and D. C. Parris, eds. *The geology and paleontology of the Late Cretaceous marine deposits of the Dakotas*. Geological Society of America Special Paper 427:71–83.
- Patterson, W. P. 1999. Oldest isotopically characterized fish otoliths provide insight to Jurassic continental climate of Europe. *Geology* 27:199–202.
- Pearce, N. J. G., W. T. Perkins, J. A. Westgate, M. P. Gorton, S. E. Jackson, C. R. Neal, and S. P. Chenery. 1997. A compilation of new and published major and trace element data for NIST SRM 610 and NIST SRM 612 glass reference materials. *Geostandards and Geoanalytical Research* 21:115–144.
- Poulain, C., A. Lorrain, R. Mas, D. P. Gillikin, F. Dehairs, R. Robert, and Y. M. Pualet. 2010. Experimental shift of diet and DIC stable carbon isotopes: influence on shell  $\delta^{13}\text{C}$  values in the Manila clam *Ruditapes philippinarum*. *Chemical Geology* 272:75–82.
- Pucéat, E., C. Lécuyer, S. M. F. Sheppard, G. Dromart, S. Reboulet, and P. Grandjean. 2003. Thermal evolution of Cretaceous Tethyan marine waters inferred from oxygen isotope composition of fish tooth enamels. *Paleoceanography* 18:1–12.
- Pucéat, E., C. Lécuyer, Y. Donnadiou, P. Naveau, H. Cappetta, G. Ramstein, B. T. Huber, and J. Kriwet. 2007. Fish tooth  $\delta^{18}\text{O}$  revising Late Cretaceous meridional upper ocean water temperature gradients. *Geology* 35:107–110.
- Rau, G. H., A. J. Mearns, D. R. Young, R. J. Olson, H. A. Schafer, and I. R. Kaplan. 1983. Animal  $^{13}\text{C}/^{12}\text{C}$  correlates with trophic level in pelagic food webs. *Ecology* 64:1314–1318.
- Rey, K., R. Amiot, F. Fouré, F. Abdala, F. Fluteau, N.-E. Jalil, B. S. Rubidge, R. M. Smith, S. J. Steyer, P. A. Viglietti, X. Wang, and C. Lécuyer. 2017. Oxygen isotopes suggest elevated thermometabolism within multiple Permo-Triassic therapsid clades. *eLife* 6:1–25.
- Rinaldi, C. A., A. Massabie, J. Morelli, H. L. Rosenman, and R. A. Del Valle. 1978. Geología de la isla Vicecomodoro Marambio. Instituto Antártico Argentino, Contribución 217, Buenos Aires.
- Robbins, J. A., K. M. Ferguson, M. J. Polcyn, and L. L. Jacobs. 2008. Application of stable carbon isotope analysis to mosasaur ecology. Pp. 123–130 *in* M. J. Everhart, ed. *Proceedings of the Second Mosasaur Meeting*. Fort Hays State University, Hays, Kans.
- Rogers, R. R., H. C. Fricke, V. Addona, R. R. Canavan, C. N. Dwyer, C. L. Harwood, A. E. Koenig, R. Murray, J. T. Thole, and J. Williams. 2010. Using laser ablation-inductively coupled plasma-mass spectrometry (LA-ICP-MS) to explore geochemical taphonomy of vertebrate fossils in the upper cretaceous two medicine and Judith River formations of Montana. *Palaios* 25:183–195.
- Schulp, A. S., H. B. Vonhof, J. H. J. L. van der Lubbe, R. Janssen, and R. R. van Baal. 2013. On diving and diet: resource partitioning in type-Maastrichtian mosasaurs. *Netherlands Journal of Geosciences* 92:165–170.
- Schulp, A. S., R. Janssen, R. R. van Baal, J. W. M. Jagt, E. W. A. Mulder, and H. B. Vonhof. 2017. Stable isotopes, niche partitioning and the paucity of elasmosaur remains in the Maastrichtian type area. *Netherlands Journal of Geosciences* 96:29–33.
- Séon, N., R. Amiot, J. E. Martin, M. T. Young, H. Middleton, F. Fouré, L. Picot, X. Valentin, and C. Lécuyer. 2020. Thermophysiology of Jurassic marine crocodylomorphs inferred from the oxygen isotope composition of their tooth apatite. *Philosophical Transactions of the Royal Society of London B* 375:20190139.
- Shackleton, N. J., and J. P. Kennett. 1976. Paleotemperature history of the Cenozoic and the initiation of Antarctic glaciation: oxygen and carbon isotope analyses in DSDP sites 277, 279 and 281. *Initial Reports of the Deep Sea Drilling Project* 29:743–755.
- Sheldon, A. 1997. Ecological implications of mosasaur bone microstructure. Pp. 333–354 *in* J. M. Callaway and E. L. Nicholls, eds. *Ancient marine reptiles*. Academic Press, San Diego.
- Shields, G. A., and G. E. Webb. 2004. Has the REE composition of seawater changed over geological time? *Chemical Geology* 204:103–107.
- Strganac, C., L. L. Jacobs, M. J. Polcyn, K. M. Ferguson, O. Mateus, A. Olimpio Gonçalves, M.-L. Morais, and T. da S. Tavares. 2015. Stable oxygen isotope chemostratigraphy and paleotemperature regime of mosasaurs at Bentiaba, Angola. *Netherlands Journal of Geosciences* 94:137–143.
- Suarez, C. A., G. L. Macpherson, L. A. González, and D. E. Grandstaff. 2010. Heterogeneous rare earth element (REE) patterns and concentrations in a fossil bone: implications for the use of REE in vertebrate taphonomy and fossilization history. *Geochimica et Cosmochimica Acta* 74:2970–2988.
- Tejada-Lara, J. V., B. J. MacFadden, L. Bermudez, G. Rojas, R. Salas-Gismondi, and J. J. Flynn. 2018. Body mass predicts isotope enrichment in herbivorous mammals. *Proceedings of the Royal Society of London B* 285:1–10.
- Tobin, T. S., and P. D. Ward. 2015. Carbon isotope ( $\delta^{13}\text{C}$ ) differences between Late Cretaceous ammonites and benthic mollusks from Antarctica. *Palaeogeography, Palaeoclimatology, Palaeoecology* 428:50–57.
- Tobin, T. S., P. D. Ward, E. J. Steig, E. B. Olivero, I. A. Hilburn, R. N. Mitchell, M. R. Diamond, T. D. Raub, and J. L. Kirschvink.

2012. Extinction patterns,  $\delta^{18}\text{O}$  trends, and magnetostratigraphy from a southern high-latitude Cretaceous–Paleogene section: links with Deccan volcanism. *Palaeogeography, Palaeoclimatology, Palaeoecology* 350–352:180–188.
- Trueman, C. N., and M. J. Benton. 1997. A geochemical method to trace the taphonomic history of reworked bones in sedimentary settings. *Geology* 25:263–266.
- Trueman, C. N., and N. Tuross. 2002. Trace elements in recent and fossil bone apatite. *Reviews in Mineralogy and Geochemistry* 48:489–521.
- Trueman, C. N., A. K. Behrensmeyer, R. Potts, and N. Tuross. 2006. High-resolution records of location and stratigraphic provenance from the rare earth element composition of fossil bones. *Geochimica et Cosmochimica Acta* 70:4343–4355.
- Trueman, C. N., L. Kocsis, M. R. Palmer, and C. Dewdney. 2011. Fractionation of rare earth elements within bone mineral: a natural cation exchange system. *Palaeogeography, Palaeoclimatology, Palaeoecology* 310:124–132.
- Tütken, T., T. W. Vennemann, and H. U. Pfretzschner. 2008. Early diagenesis of bone and tooth apatite in fluvial and marine settings: constraints from combined oxygen isotope, nitrogen and REE analysis. *Palaeogeography, Palaeoclimatology, Palaeoecology* 266:254–268.
- Uliana, M. A., and K. T. Biddle. 1988. Mesozoic–Cenozoic paleogeographic and geodynamic evolution of southern South America. *Revista Brasileira de Geociências* 18:172–190.
- Vennemann, T. W., E. Hegner, G. Cliff, and G. W. Benz. 2001. Isotopic composition of recent shark teeth as a proxy for environmental conditions. *Geochimica et Cosmochimica Acta* 65:1583–1599.
- Vennemann, T. W., H. C. Fricke, R. E. Blake, J. R. O’Neil, and A. Colman. 2002. Oxygen isotope analyses of phosphates: a comparison of techniques for analysis of  $\text{Ag}_3\text{PO}_4$ . *Chemical Geology* 185:321–336.
- Villamarín, F., T. D. Jardine, S. E. Bunn, B. Marioni, and W. E. Magnusson. 2018. Body size is more important than diet in determining stable-isotope estimates of trophic position in crocodylians. *Scientific Reports* 8:1–11.
- Wada, E., M. Terazaki, Y. Kabaya, and T. Nemoto. 1987.  $^{15}\text{N}$  and  $^{13}\text{C}$  abundances in the Antarctic Ocean with emphasis on the biogeochemical structure of the food web. *Deep-Sea Research* 34:829–841.
- Wang, Y., and T. E. Cerling. 1994. A model of fossil tooth and bone diagenesis: implications for paleodiet reconstruction from stable isotopes. *Palaeogeography, Palaeoclimatology, Palaeoecology* 107:281–289.
- Withers, P. C. 1992. *Comparative animal physiology*. Saunders College Publishing, Philadelphia.
- Woelders, L., J. Vellekoop, D. Kroon, J. Smit, S. Casadio, M. B. Prámparo, J. Dinarès-Turell, F. Peterse, A. Sluijs, J. T. M. Lenaerts, and R. P. Speijer. 2017. Latest Cretaceous climatic and environmental change in the South Atlantic region. *Paleoceanography* 32:466–483.
- Wright, J., H. Schrader, and W. T. Holser. 1987. Paleoredox variations in ancient oceans recorded by rare earth elements in fossil apatite. *Geochimica et Cosmochimica Acta* 51:631–644.
- Yamashita, M., T. Konishi, and T. Sato. 2012. Diversity of diving behavior of mosasaurs (Squamata: Mosasauridae) inferred from optical system. *Journal of Vertebrate Paleontology* 32:197.
- Zachos, J. C., D. Stott, and K. C. Lohmann. 1994. Evolution of early Cenozoic marine temperatures. *Paleoceanography and Paleoclimatology* 9:353–387.
- Zazzo, A., C. Lécuyer, S. M. F. Sheppard, P. Grandjean, and A. Mariotti. 2004. Diagenesis and the reconstruction of paleoenvironments: a method to restore original  $\delta^{18}\text{O}$  values of carbonate and phosphate from fossil tooth enamel. *Geochimica et Cosmochimica Acta* 68:2245–2258.
- Zhang, L., W. W. Hay, C. Wang, and X. Gu. 2019. The evolution of latitudinal temperature gradients from the latest Cretaceous through the present. *Earth-Science Reviews* 189:147–158.